Cooperative control of heterogeneous multi-agent systems under spatiotemporal constraints*

Fei Chen[a,*], Mayank Sewlia[a], Dimos V. Dimarogonas[a]

[a]*Division of Decision and Control Systems, KTH Royal Institute of Technology, SE-100 44, Stockholm, Sweden*

Abstract

A current trend in research on multi-agent control systems is to consider high-level task specifications that go beyond traditional control objectives and take into account the heterogeneity of each agent in the system, i.e., the different capabilities of the agents in terms of actuation, sensing, communication and computation. This article provides an overview of our work on the problem of control of heterogeneous multi-agent systems under both spatial and temporal constraints as well as our perspective on the challenges and open problems associated with the consideration of such spatiotemporal constraints. Initially, we review a set of control strategies introduced by the authors addressing the satisfaction of cooperative tasks such as formation control as well as individual objectives such as reference tracking. The satisfaction of those objectives is ensured using prescribed performance control. Building upon these approaches we then review recent results on control under high-level spatiotemporal objectives expressed in Signal Temporal Logic, a formal language that allows to express complex spatial tasks that must be satisfied within pre-defined deadlines. Theoretical results considering multi-agent systems with various capabilities under spatiotemporal constraints are presented.

Keywords: Heterogeneous multi-agent system; Leader-follower network; Spatiotemporal constraints; Prescribed performance control;

1. Introduction

Cooperative control [1] of multi-agent systems has emerged as a popular research area due to its wide applications in various domains such as manufacturing, robotics, social networks [2], network security [3], intelligent transportation systems [4], and more. The overarching themes encompass consensus [5], formation [6], flocking [7], coverage control [8] and so on. The principal approach entails integrating tools from single-agent control into a multi-agent framework, considering the distinct properties of the involved agents. These properties encompass diverse agent dynamics, actuation capabilities, as well as communication and sensing limitations.

Transient control for heterogeneous multi-agent systems. In addition to fulfilling the classical stabilization objectives in multi-agent systems, a mobile robot team may encounter the need to address additional transient behaviors arising from performance requirements or spatiotemporal constraints. Examples include collision avoidance within the workspace or between agents. Recent research has extended its focus to consider these transient constraints while steering multi-agent systems using distributed control laws towards target average consensus [9] or platoon formation [10]. However, these distributed control laws are designed for all agents which may be redundant and costly. This is because achieving target consensus or formation, along with fulfilling transient behavior, may be efficiently accomplished by steering a subset of agents through appropriately designed local control strategies, while the remaining agents adhere to standard distributed control protocols. For instance, in applications like multi-robot coordination or drone formation, a subset of robots may possess advanced capabilities, such as communication, computation or actuation. These advanced robots can act as leaders, guiding the entire group to fulfill the tasks. Another scenario is observed in multi-vehicle platooning, where certain vehicles may be designated as leaders to guide follower vehicles, reducing overall costs. Additionally, there are fascinating natural occurrences involving leader-follower network, such as fish swarming and bird flocking, in which the follower entity can conserve energy by simply following its leader. Therefore, we instead consider in this article a heterogeneous, leader-follower approach, in which a selected set of agents with advanced actuation, computation and communication capabilities, namely the leaders, are responsible for guiding the whole agent group to fulfill the stabilization objectives while satisfying the transient constraints.

Cooperative control under high-level specifica-

*This work was supported by the ERC Consolidator Grant LEAFHOUND, the Swedish Research Council (VR) and the Knut och Alice Wallenberg Foundation (KAW).

*Corresponding author

Email addresses: fchen@kth.se (Fei Chen), sewlia@kth.se (Mayank Sewlia), dimos@kth.se (Dimos V. Dimarogonas)

tions. So far, our discussion has focused on controlling multi-agent systems with the aim of stabilizing the system to an equilibrium. However, many tasks in various applications are more complicated and cannot be simply cast as a traditional control objective. Instead, they require higher level specifications. For instance, in certain industrial warehouses, a group of robots might be assigned a repetitive task at a higher level. This task could involve inspecting specific areas and collaboratively transporting products. Such tasks may also present space constraints, such as collision avoidance against obstacles in the workspace or collision avoidance among the robots, as well as time constraints, for example, completing certain time-critical tasks within a given deadline. Therefore, within the heterogeneous leader-follower framework, the selected leader agents are responsible for leading the entire agent group in implementing the high-level spatiotemporal task specification in a decentralized and collaborative manner. Temporal logics [11] show such ability to express more complex and high-level task specifications that expand beyond the standard control objectives. Compared with the formal methods [12] based approaches for single agent systems, e.g., [13], the consideration in a multi-agent setup can include more real world applications such as multi-robot coordination and transportation systems. The multi-agent case requires further analysis of the couplings with respect to dynamics or task specifications. Signal Temporal Logic (STL) [14], which is based on continuous-time signals, can be used to deal with quantitative spatiotemporal constraints for multi-agent systems since it allows both time and space constraints.

Applications and research extensions. In practical applications (e.g., cooperative control of mobile robots), a group of agents may showcase different dynamics, actuation or computation capabilities, as well as communication and sensing limitations. How to intelligently utilize their diverse capabilities to lower the cost or avoid redundant effort has become significantly more crucial. In particular, the research within heterogeneous leader-follower framework finds applications in various domains, including multi-vehicle platooning. This involves designing leader vehicle controllers to ensure collision avoidance and maintain connectivity for the entire platoon. In addition, it encompasses multi-robot coordination, involving formation control or even more complex task planning for robot teams under spatiotemporal constraints, where only the controllers of the leader robots are developed. Furthermore, the framework enables collaborative manipulation, involving grasping and transporting objects in a collaborative leader-follower manner while satisfying the transient constraints. All these tasks are assigned to the available leader agents, demonstrating both a distributed and scalable nature. Moreover, analyzing the topology of the leader-follower network to ensure transient constraints poses a significant challenge. However, it brings forth several advantages in diverse areas, including addressing leader selection problems amidst transient constraints, studying the network's robustness in terms of agent failures, and exploring network reconfigurations.

Overview of our research. In this article, we provide an overview of our work on the problem of cooperative control of heterogeneous multi-agent systems under both spatial and temporal constraints, in which a leader-follower framework is treated as a specific class of heterogeneous multi-agent systems. In the first part of this article, we focus on a heterogeneous leader-follower framework and present a systematic approach for designing the leader controllers only to ensure the convergence of the entire team to the desired equilibrium while simultaneously adhering to transient constraints. The satisfaction of the transient constraints is ensured using prescribed performance control (PPC) [15], which was initially introduced to prescribe the evolution of the system output or tracking error within certain predefined transient bounds. In particular, the transient constraints are imposed to the whole team but the freedom for control design is only assigned to the leaders. Additionally, we investigate the topological conditions on the heterogeneous leader-follower networks such that the target objective can be achieved within the prescribed transient constraints. The second part of this article focuses on cooperative control and task planning of heterogeneous multi-agent systems under spatiotemporal logic tasks. Such complex and high-level tasks are represented by STL specifications that characterize both time and space constraints. For the heterogeneous leader-follower multi-agent system, which can be treated as a composition of several leader-follower subsystems through their coupled dynamics, we also consider how to tackle the couplings with respect to the dynamics and local STL specifications. For each subsystem, only the leaders know the STL specifications and are designed to fulfill the tasks, while the followers are indirectly guided through their dynamic couplings with the controlled leaders without any further control and knowledge of the STL tasks. Next, we present results pertaining to the cooperative manipulation problem, wherein STL tasks are defined with respect to the manipulated object. We account for uncertain dynamics of both the agents and the object. In addition, we offer insights into how sampling-based planning algorithms can be utilized to generate trajectories that satisfy STL tasks. The organization of the paper is graphically depicted in Figure. 1.

2. Related work

2.1. Heterogeneous leader-follower multi-agent systems

In the context of heterogeneous leader-follower multi-agent systems, extensive research has been conducted on single leader cases. In such cases, the single leader acts as a reference for the followers, and efforts are made to design all the remaining followers to achieve various objectives such as consensus and formation. For instance, the

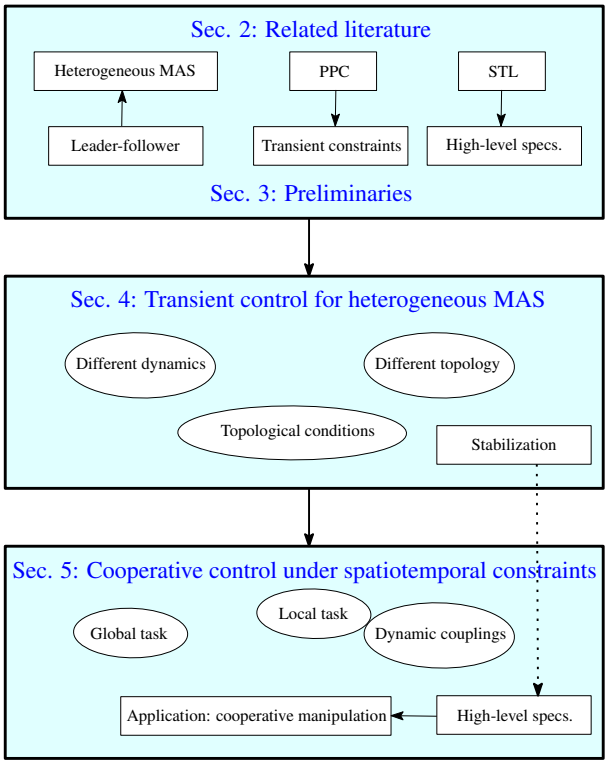

Figure 1: Organization of the paper.

authors in [16] tackle the leader-follower multi-agent consensus problem, considering a time-invariant communication topology with general linear node dynamics. Another study in [17] addresses the leader-follower consensus tracking problem for multi-agent systems with identical general linear dynamics and unknown external disturbances. Distributed control for leader-follower multi-agent systems under partial and noisy measurements and time-varying directed network topology is explored in [18]. In [19], the authors propose distributed leader-follower control algorithms for linear multi-agent systems based on output regulation theory. It is noteworthy that our focus shifts to a distinct and more general heterogeneous leader-follower framework, where we allow an arbitrary number of leaders and we solely design these leader controllers to steer the entire system towards achieving specific objectives. The related literature, for example, the study in [20] addresses containment in leader-follower networks using an undirected switching graph topology, assuming static leaders. The authors in [21] delve into optimal control for multi-agent systems with multiple leaders, while [22] contributes to investigate the robustness of leader-follower consensus dynamics in the presence of disturbances and time delays.

We then provide a summary of the primary research conducted within such general and heterogeneous leader-follower setting, categorizing it into two main schemes: controllability of leader-follower multi-agent systems and leader selection problems.

Controllability. The controllability of leader-follower multi-agent systems was initially explored in [23]. This study derives conditions on the network topology to ensure that the network can be controlled by a specific agent acting as a leader. In [24, 25], the authors identify necessary conditions for the controllability of corresponding leader-follower networks using equitable partitions of graphs. Controllability conditions for leader-follower multi-agent systems with double integrator dynamics and their connection with graph topology properties are addressed in [26]. Controllability of multi-agent systems defined by undirected signed graphs through almost equitable partition is investigated in [27], and a necessary condition for the controllability of the network is provided. In [21], a sufficient controllability condition together with optimal control techniques for driving the leader-follower multi-agent systems between specific positions are developed. Several works, including [28, 29, 30], focus on investigating lower or upper bounds for controllable subspaces of leader-follower networks, which is valuable for leader selection problems, determining the smallest set of leaders that must be manipulated to achieve overall system controllability. In [31], the authors explore graph controllability classes, specifically the classes of essentially controllable, completely uncontrollable, and conditionally controllable graphs. Another noteworthy work [32] on leader selection with controllability guarantees demonstrates that the dimension of the controllable subspace remains invariant under the addition or removal of edges between leaders, and a controllable structure can be obtained via connecting the leaders of disjoint sub-graphs that are all controllable.

Leader selection. Leader selection aims to effectively choose a group of leaders with the goal of ensuring controllability in leader-follower multi-agent systems or maximizing a system performance metric. This performance metric encompasses energy-related metrics, robustness metrics, transient performance metrics, and more. A considerable body of literature has been dedicated to studying the controllability of leader-follower multi-agent systems, as summarized in the previous paragraph, such as in works like [27, 25, 29]. While some of these studies do not explicitly address leader selection problems, they establish conditions on the graph topology of the leader-follower multi-agent networks, which implicitly propose the criteria for choosing leaders among the agents to ensure certain conditions, such as specific matrix properties. Other works delve into the explicit problem of selecting leaders among the agents to optimize the performance of the leader-follower multi-agent system based on predefined metrics. For example, in [33] various standard measures of controllability defined based on the control Gramian are utilized as the performance metric. The leader selection problem is explicitly addressed in [34], where the authors consider a setting in which leaders maintain an identical, constant value, and followers are subject to stochastic disturbance. In this context, k leaders are selected to minimize the steady-state variance of the derivation. Efficient algorithms are proposed in [35] to select k leaders based

on performance metrics like coherence and convergence rate in specific path graphs and ring graphs. In another study [36], the authors investigate the optimal assignment of a predetermined number of leaders to ensure optimal performance measured in terms of the $\mathcal{H}_2$ norm of the network. The leader selection for tracking and the task of driving the centroid of the agents to a given reference point is considered in [37].

2.2. Prescribed performance control and funnel control

Prescribed Performance Control (PPC) was initially introduced in [15] with the objective of prescribing the evolution of the system output or tracking error within predefined bounds. For instance, in [9], an agreement protocol is proposed to attain the specified performance for a combined error in positions and velocities. This protocol is designed for multi-agent systems with double integrator dynamics. On the other hand, PPC for multi-agent average consensus with single integrator dynamics is introduced in [38] . In [39], the authors address the formation control problem for nonlinear multi-agent systems, considering prescribed performance guarantees and connectivity constraints. The authors in [40] employ PPC for the formation of large vehicle platoons. The goal is to prevent connectivity breaks and collisions with neighboring vehicles. Multi-agent coordination with second-order uncertain Lagrangian dynamics to ensure collision avoidance and connectivity maintenance is addressed in [41]. The authors in [42] concentrate on robot joint position control in order to provide guaranteed performance and to bound the error within certain region for both regulation and tracking problems. In [43], an output feedback control protocol for leader-follower synchronization problem is proposed, where second-order, nonlinear multi-agent systems with unknown dynamics are assumed. In [44], PPC is applied to solve the regulation problem for the unicycle model. The work in [45] tackles the tracking problem of unknown, robustly stabilizable, multi-input multi-output, affine in control, nonlinear systems. The distance and orientation formation control of rigid bodies is explored in [46], where PPC is employed to ensure the satisfaction of inter-agent distance constraints. The application of PPC under temporal logic specifications is discussed in [47, 48, 49]. In [47], the authors investigate PPC for nonlinear systems subject to a subset of signal temporal logic specifications. Meanwhile, a distributed cooperative manipulation problem that satisfies a given metric interval temporal logic (MITL) specification under the PPC framework is explored in [48]. In [49], a distributed hybrid control strategy is proposed for multi-agent systems with contingent temporal tasks and prescribed formation constraints.

Funnel control, akin to PPC, was initially introduced in the context of tracking problems, as detailed in [50, 51, 52]. In [53], the authors utilize funnel control for uncertain nonlinear systems that have arbitrary strict relative degree and input-to-state stable internal dynamics, while funnel control for linear or nonlinear systems with relative degree one or two are investigated in [54, 55], where [54] also considers input saturation. Input saturation is further investigated in [56, 57, 58]. Funnel control for output tracking control of uncertain nonlinear systems with arbitrary known relative degree is presented in [59]. These works also highlight the model-free properties of funnel-based control. Synchronization of heterogeneous multi-agent systems via funnel control is studied in [60, 61, 62]. Some other noteworthy contributions delve into optimization-based funnel control using model predictive control [63, 64]. In terms of practical applications, funnel control finds utility in various domains such as chemical reactor models [58], electrical circuits [65], and cruise control [66].

2.3. Signal temporal logic

Temporal logics, such as linear temporal logic (LTL) [67] and signal temporal logic (STL) [68] show the ability to express more complex and high-level task specifications that expand beyond standard control objectives, such as stabilization to the desired equilibria. STL, based on continuous-time signals, incorporates the additional feature of formulating both time and space constraints. This characteristic provides the potential to address quantitative transient constraints for multi-agent systems. Various robustness metrics for STL are explored in [69, 70, 71, 72, 73, 74]. Current approaches addressing control synthesis under STL specifications mainly involve barrier function methods [75, 76, 77, 78, 79, 80], optimization-based methods [81, 82, 78, 83], sampling-based methods [84], and learning-based methods [85, 86, 87, 88, 89, 90]. In [91], an optimization-based approach for robot planning, monitoring, and self-correction problems under STL specifications is presented. This approach is further solved using mixed-integer linear programming. The study in [92] proposes a method to compute the quantitative semantics of STL formulas using computation graphs. STL specifications with integral and derivative predicates are investigated in [93]. The coordination problem of heterogeneous multi-agent systems under STL tasks with integral predicates is considered in [94].Additionally, [95] introduces a funnel-based feedback control strategy for a single system under a fragment of STL specifications, while the considerations in a multi-agent setup are discussed in [96].

3. Preliminaries

3.1. Graph theory

An undirected graph [97] $\mathcal{G} = (\mathcal{V}, \mathcal{E})$ is comprised of the vertices set $\mathcal{V} = \{1, 2, \ldots, n\}$ and the edges set $\mathcal{E} = \{(i, j) \in \mathcal{V} \times \mathcal{V} \mid j \in \mathcal{N}_i\}$ indexed by $e_1, e_2, \ldots, e_m$, where $m = |\mathcal{E}|$ is the number of edges and $\mathcal{N}_i$ denotes the agents in the neighborhood of agent i that can communicate with i. For an edge $e_k = (i, j)$, $\mathbf{v}(e_k) = \{i, j\}$ is the set composed of the vertices of e_k. The *adjacency matrix* $\mathbb{A}$ of

$\mathcal{G}$ is the $n \times n$ symmetric matrix whose elements a_{ij} are given by $a_{ij} = 1$, if $(i,j) \in \mathcal{E}$, and $a_{ij} = 0$, otherwise. The degree of vertex i is defined as $d_i = \sum_{j \in \mathcal{N}_i} a_{ij}$. Then, the *degree matrix* is $\Delta = \text{diag}(d_1, d_2, \ldots, d_n)$. The *graph Laplacian* of $\mathcal{G}$ is $L = \Delta - \mathbb{A}$. A *path* is a sequence of edges connecting two distinct vertices. A graph is *connected* if there exists a path between any pair of vertices. By assigning an orientation to each edge of $\mathcal{G}$ we can define the *incidence matrix* $D = D(\mathcal{G}) = [d_{ij}] \in \mathbb{R}^{n \times m}$. The rows of D are indexed by the vertices and the columns are indexed by the edges with $d_{ij} = 1$ if the vertex i is the head of the edge (i,j), $d_{ij} = -1$ if the vertex i is the tail of the edge (i,j) and $d_{ij} = 0$ otherwise. Based on the incidence matrix, the graph Laplacian of $\mathcal{G}$ can be described as $L = DD^T$. In addition, $L_e = D^T D$ is the so-called *edge Laplacian* [97] and c_{ij} denotes the elements of L_e.

3.2. Prescribed performance control

In the heterogeneous leader-follower framework, we use PPC to prescribe the evolution of the signal $\bar{x}_i(t)$ within a predefined region described as

$$-\rho_{\bar{x}_i}(t) < \bar{x}_i(t) < \rho_{\bar{x}_i}(t). \tag{1}$$

Here $\rho_{\bar{x}_i} : \mathbb{R}_+ \to \mathbb{R}_+ \setminus \{0\}, i = 1, 2, \ldots, m$ are positive, smooth and nonincreasing performance functions that introduce the predefined bounds for $\bar{x}_i(t)$. One example choice is

$$\rho_{\bar{x}_i}(t) = (\rho_{\bar{x}_{i0}} - \rho_{\bar{x}_{i\infty}})e^{-l_{\bar{x}_i} t} + \rho_{\bar{x}_{i\infty}}, \tag{2}$$

where $\rho_{\bar{x}_{i0}}, \rho_{\bar{x}_{i\infty}}$ and $l_{\bar{x}_i}$ are positive parameters and $\rho_{\bar{x}_{i\infty}} = \lim_{t\to\infty} \rho_{\bar{x}_i}(t)$ represents the maximum allowable tracking error at steady state.

Normalizing $\bar{x}_i(t)$ with respect to the performance function $\rho_{\bar{x}_i}(t)$, we define the modulated error as $\hat{\bar{x}}_i(t)$ and the corresponding prescribed performance region $\mathcal{D}_{\bar{x}_i}$ as:

$$\hat{\bar{x}}_i(t) = \frac{\bar{x}_i(t)}{\rho_{\bar{x}_i}(t)}, \tag{3}$$

$$\mathcal{D}_{\bar{x}_i} \triangleq \{\hat{\bar{x}}_i : \hat{\bar{x}}_i \in (-1, 1)\}. \tag{4}$$

Then, the modulated error is transformed through a transformation function $T_{\bar{x}_i}$ that defines the smooth and strictly increasing mapping $T_{\bar{x}_i} : \mathcal{D}_{\bar{x}_i} \to \mathbb{R}$. One example choice is

$$T_{\bar{x}_i}(\hat{\bar{x}}_i) = \ln\left(\frac{1 + \hat{\bar{x}}_i}{1 - \hat{\bar{x}}_i}\right). \tag{5}$$

The transformed error is then defined as

$$\varepsilon_{\bar{x}_i}(\hat{\bar{x}}_i) = T_{\bar{x}_i}(\hat{\bar{x}}_i). \tag{6}$$

It can be verified that if the transformed error $\varepsilon_{\bar{x}_i}(\hat{\bar{x}}_i)$ is bounded, then the modulated error $\hat{\bar{x}}_i$ is constrained within the region (4). This also implies the error $\bar{x}_i$ evolves within the predefined performance bounds (1). Differentiating (6) with respect to time, we derive

$$\dot{\varepsilon}_{\bar{x}_i}(\hat{\bar{x}}_i) = \mathcal{J}_{T_{\bar{x}_i}}(\hat{\bar{x}}_i, t)[\dot{\bar{x}}_i + \alpha_{\bar{x}_i}(t)\bar{x}_i] \tag{7}$$

where

$$\mathcal{J}_{T_{\bar{x}_i}}(\hat{\bar{x}}_i, t) \triangleq \frac{\partial T_{\bar{x}_i}(\hat{\bar{x}}_i)}{\partial \hat{\bar{x}}_i} \frac{1}{\rho_{\bar{x}_i}(t)} > 0 \tag{8}$$

$$\alpha_{\bar{x}_i}(t) \triangleq -\frac{\dot{\rho}_{\bar{x}_i}(t)}{\rho_{\bar{x}_i}(t)} > 0 \tag{9}$$

are the normalized Jacobian of the transformed function $T_{\bar{x}_i}$ and the normalized derivative of the performance function, respectively.

3.3. Signal temporal logic

Signal temporal logic (STL) [14] consists of predicates $\mu : \mathbb{R}^n \to \mathbb{B}$ which are obtained by evaluating a continuously differentiable predicate function $h : \mathbb{R}^n \to \mathbb{R}$ and assigning the respective true or false boolean value as follows:

$$\mu = \begin{cases} \top, & h(x) \geq 0; \\ \bot, & h(x) < 0, \end{cases} \tag{10}$$

where $x \in \mathbb{R}^n$. The STL syntax is defined as

$$\phi ::= \top \mid \mu \mid \neg\phi \mid \phi_1 \wedge \phi_2 \mid \phi_1 \mathrm{U}_{[a,b]} \phi_2, \tag{11}$$

where ϕ_1, ϕ_2 are STL formulas and $\neg, \wedge, \mathrm{U}_{[a,b]}$ are the respective negation, conjunction, until operators with $0 \leq a \leq b < \infty$. Define "eventually" operator and "always" operator as $\mathrm{F}_{[a,b]}\phi := \top \mathrm{U}_{[a,b]}\phi$ and $\mathrm{G}_{[a,b]}\phi := \neg \mathrm{F}_{[a,b]} \neg\phi$, respectively. For a continuous-time signal $x : \mathbb{R}_{\geq 0} \to \mathbb{R}^n$, $(x,t) \models \phi$ denotes the satisfaction relation, which holds if x satisfies ϕ at time t. Robust semantics have been introduced in [98] in order to quantify how robustly the signal x satisfies the STL formula ϕ at time t. Space robustness semantics [99] for STL are defined as follows:

$$\varrho^{\mu}(x,t) := h(x(t));$$

$$\varrho^{\neg\phi}(x,t) := -\varrho^{\phi}(x,t);$$

$$\varrho^{\phi_1 \wedge \phi_2}(x,t) := \min(\varrho^{\phi_1}(x,t), \varrho^{\phi_2}(x,t));$$

$$\varrho^{\mathrm{F}_{[a,b]}\phi}(x,t) := \max_{t_1 \in [t+a, t+b]} \varrho^{\phi}(x, t_1);$$

$$\varrho^{\mathrm{G}_{[a,b]}\phi}(x,t) := \min_{t_1 \in [t+a, t+b]} \varrho^{\phi}(x, t_1).$$

Note that it holds that $(x,t) \models \phi$ if $\varrho^{\phi}(x,t) > 0$.

3.4. Cooperative manipulation

Cooperative manipulation involves multiple robots working together to handle an object. This approach offers advantages in enabling the manipulation of heavier objects when the load exceeds the carrying capacity of a single robot. Consider N robotic agents rigidly grasping an object, as illustrated in Figure 2. Each robot possesses a base reference frame A_i and an end-effector's reference frame E_i, where $i \in 1, \ldots, N$. The object being grasped has its own reference frame O, centred at its centre of mass. The robot-object system operates within a workspace $\mathcal{W} \subset \mathbb{R}^3$, which includes an inertial reference frame I. The rigid grasping ensures a fixed distance $p_{i/o}$

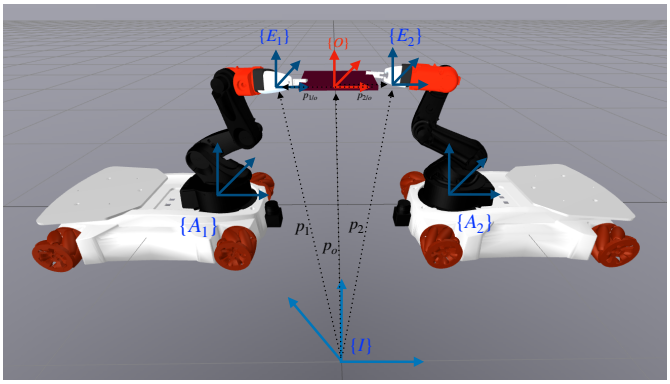

Figure 2: Two arms rigidly grasping an object

between the end-effector frame of robot i to the object's reference frame, as depicted in Figure 2.

In the following, we describe the agents' and objects' dynamics and also present the coupled dynamics.

3.4.1. Agent dynamics

Let the joint-space variables of agent $i \in \mathcal{N}$ be denoted by $q_i \in \mathbb{R}^{n_i}$, where n_i is greater than or equal to 6. The position and Euler-angles of the end-effector i are represented as $p_i \in \mathbb{R}^3$ and $\eta_i \in \mathbb{T}^3$, respectively. Additionally, the velocity of the end-effector of agent i is represented as $v_i \in \mathbb{R}^6$, and is defined by $v_i = [\dot{p}_i^\top, \omega_i^\top]^\top$, where $\omega_i \in \mathbb{R}^3$ is the respective angular velocity. The relationship between v_i and q_i is established through the kinematic Jacobian matrix $J_i : \mathbb{R}^{n_i} \times \mathbb{R}^{6\times n_i}$ as $v_i = J_i(q_i)\dot{q}_i$. As common in literature, we assume that the agent operates away from its kinematic singularities leading to well-defined task space dynamics [100]

$$M_i(q_i)\dot{v}_i + C_i(q_i, \dot{q}_i)v_i + g_i(q_i) + w_i(q_i, \dot{q}_i, t) = u_i - \lambda_i \quad (12)$$

where $M_i : \mathbb{R}^{n_i} \to \mathbb{R}^{6\times 6}$ is the task-space positive definite mass matrix, $C_i : \mathbb{R}^{2n_i} \to \mathbb{R}^{6\times 6}$ the task-space Coriolis matrix, $g_i : \mathbb{R}^{n_i} \to \mathbb{R}^6$ the task-space gravity vector, $w_i : \mathbb{R}^{2n_i} \times \mathbb{R}_{\geq 0} \to \mathbb{R}^6$ represents model uncertainties and bounded external disturbances, $u_i \in \mathbb{R}^6$ is the task-space input wrench and $\lambda_i \in \mathbb{R}^6$ is the generalized force vector that agent i exerts on the object. We assume that all dynamic terms $M_i(\cdot)$, $C_i(\cdot)$, $g_i(\cdot)$, $w_i(\cdot)$ are *unknown* in this work. The vector fields $M_i(\cdot)$, $C_i(\cdot)$, $g_i(\cdot)$, are continuously differentiable [100], and we further assume that $w_i(q_i, \dot{q}_i, t)$ is continuous in q_i and $\dot{q}_i$ for each fixed $t \geq 0$, and uniformly bounded in t for each fixed $(q_i, \dot{q}_i) \in \mathbb{R}^{2n_i}$. An agent only has access to to its end effector's pose (p_i, η_i) through the forward kinematics. The dynamics (12) can be written in vector form as:

$$M(q)\dot{v} + C(q, \dot{q})v + g(q) + w(q, \dot{q}, t) = u - \lambda, \quad (13)$$

where $v = [v_1^\top, \ldots, v_N^\top] \in \mathbb{R}^{6N}$, $M = \text{diag}\{[M_i]\} \in \mathbb{R}^{6N\times 6N}$, $C = \text{diag}\{[C_i]\} \in \mathbb{R}^{6N\times 6N}$, $g = [g_1^\top, \ldots, g_N^\top]^\top \in \mathbb{R}^{6N}$, $w = [w_1^\top, \ldots, w_N^\top]^\top \in \mathbb{R}^{6N}$, $u = [u_1^\top, \ldots, u_N^\top]^\top \in \mathbb{R}^{6N}$ and $\lambda = [\lambda_1^\top, \ldots, \lambda_N^\top]^\top \in \mathbb{R}^{6N}$.

3.4.2. Object dynamics

The pose of the object's centre of mass is denoted by $\mathbf{x}_0 = [p_o^\top, \eta_o^\top]^\top \in \mathbb{M}$ where $p_o \in \mathbb{R}^3$, $\eta_o \in \mathbb{R}^3$ and the velocity by $v_o = [\dot{p}_o^\top, \omega_o^\top]^\top \in \mathbb{R}^6$ where $\omega_o \in \mathbb{R}^3$.

The dynamics of the object are given by

$$\dot{\mathbf{x}}_o = J_{o_r}^{-1}(\mathbf{x}_o)v_o, \quad (14a)$$

$$M_o(\mathbf{x}_o)\dot{v}_o + C_o(\mathbf{x}_o, v_o)v_o + g_o(\mathbf{x}_o) + w_o(t) = \lambda_o \quad (14b)$$

where $M_o : \mathbb{M} \to \mathbb{R}^{6\times 6}$ is the positive-definite inertia matrix, $C_o : \mathbb{M} \times \mathbb{R}^6 \to \mathbb{R}^{6\times 6}$ is the Coriolis matrix, $g_o : \mathbb{M} \to \mathbb{R}^6$ is the gravity vector and $w_o : \mathbb{R}_{\geq 0} \to \mathbb{R}^6$ is a bounded vector of external disturbances. Additionally, $J_{o_r} : \mathbb{M} \to \mathbb{R}^{6\times 6}$ is the object representation Jacobian and $\lambda_o \in \mathbb{R}^6$ is the force acting on the object's center of mass. Like the object's dynamics, the terms $M_o(\cdot)$, $C_o(\cdot)$, $g_o(\cdot)$ are continuously differentiable and we assume that $w_o(t)$ is bounded. The matrix J_{o_r} and its inverse are well-defined when we assume the object's pitch angle $\theta_o \in (-\frac{\pi}{2}, \frac{\pi}{2})$. Similarly to the agent's, the object's dynamic terms $M_o(\cdot)$, $C_o(\cdot)$, $g_o(\cdot)$, $w_o(\cdot)$ and force λ_o are considered to be unknown and cannot be used in the control design.

3.4.3. Coupled dynamics

Using the fact that the force exerted by the agents is equal to the force experienced by the object, and using (12) and (14), leads us to the coupled dynamics

$$\tilde{M}(q)\dot{v}_o + \tilde{C}(q, \dot{q})v_o + \tilde{g}(q, \dot{q}) + \tilde{w}(q, t) = G^\top(q)u \quad (15)$$

where $\tilde{M}(q) = M_o(q) + G^\top(q)M(q)G(q)$, $\tilde{C}(q, \dot{q}) = C_o(q, \dot{q}) + G^\top(q)M(q)\dot{G}(q) + G^\top(q)C(q, \dot{q})G(q)$, $\tilde{g}(q, \dot{q}) = g_o(q) + G^\top(q)g(q)$ and $\tilde{w}(q, t) = w_o(t) + G^\top(q)w(q, t)$. The grasp matrix $G(q) = [J_{o_1}^\top(q_1), \ldots, J_{o_N}^\top(q_N)]^\top$ is full column rank due to grasp rigidity, where $J_{o_i} : \mathbb{R}^{n_i} \to \mathbb{R}^{6\times 6}$ is the object-to-i'th agent Jacobian

$$J_{o_i}(q_i) = \begin{bmatrix} I_3 & S(-p_{i/o}(q_i)) \\ 0_{3\times 3} & I_3 \end{bmatrix}. \quad (16)$$

The Jacobian $J_{o_i}(q_i)$, due to rigid grasps, is invertible and enables agents to calculate the object's velocity using the relation $v_i = J_{o_i}(q_i)v_o$.

4. Transient control for heterogeneous multi-agent systems

We focus on a heterogeneous leader-follower framework in this section and introduce a systematic approach to design the leader controllers exclusively. This is done to guarantee the convergence of the entire team to the desired equilibrium while also adhering to transient constraints. Notably, these transient constraints are applied to the entire team, yet the freedom for control design is only for the leaders. Firstly, we consider transient control for both first-order and second-order leader-follower multi-agent systems under tree graphs. Secondly, we extend the

findings to the first-order case under general graphs, which encompass cycles and avoid the need for tree assumptions. Furthermore, we explore the topological conditions within heterogeneous leader-follower networks to ensure that the target objective can be attained while complying with the specified transient constraints. An overview of the control objectives is presented in Subsection 4.1. We mainly focus on first-order dynamics, with an extension to second-order cases in Subsection in 4.3.

4.1. Control objectives for heterogeneous leader-follower multi-agent systems

We consider a heterogeneous leader-follower multi-agent system with vertices $\mathcal{V} = \{1, 2, \ldots, n\}$. Without loss of generality, we suppose that the first n_f agents are selected as followers while the last n_l agents are selected as leaders with respective vertices set $\mathcal{V}_F = \{1, \ldots, n_f\}$, $\mathcal{V}_L = \{n_f + 1, \ldots, n_f + n_l\}$ and $n = n_f + n_l$.

Denote $p_i \in \mathbb{R}$ as the position of agent i, where we only consider the one dimensional case, without loss of generality. Specifically, the results can be extended to higher dimensions with appropriate use of the Kronecker product. The target relative position-based formation is described as follows:

$$\mathcal{F} := \{p \mid p_i - p_j = p_{ij}^{des}, (i, j) \in \mathcal{E}\}, \tag{17}$$

where $p_{ij}^{des} := p_i^{des} - p_j^{des}, (i, j) \in \mathcal{E}$ is the desired relative position between agent i and agent j, which is constant and denoted as the difference between the absolute desired positions $p_i^{des}, p_j^{des} \in \mathbb{R}$. Here, only p_{ij}^{des} needs to be known and p_i^{des}, p_j^{des} are defined with respect to an arbitrary reference frame and do not need to be known. In the first-order case, the state evolution of each follower $i \in \mathcal{V}_F$ is governed by the first-order formation protocol:

$$\dot{p}_i = -\sum_{j \in \mathcal{N}_i} (p_i - p_j - p_{ij}^{des}), \tag{18}$$

while leader $i \in \mathcal{V}_L$ obeys the following first-order formation protocol with an assigned external input $u_i \in \mathbb{R}$:

$$\dot{p}_i = -\sum_{j \in \mathcal{N}_i} (p_i - p_j - p_{ij}^{des}) + u_i. \tag{19}$$

We denote $p = [p_1, \ldots, p_n]^T, p^{des} = [p_1^{des}, \ldots, p_n^{des}]^T \in \mathbb{R}^n$ as the respective stack vector of absolute positions and target positions and $u = [u_{n_f+1}, \ldots, u_{n_f+n_l}]^T \in \mathbb{R}^{n_l}$ is the control input vector that contains the external inputs of leader agents in (19). Denote $\bar{p} = [\bar{p}_1, \ldots, \bar{p}_m]^T$, $\bar{p}^{des} = [\bar{p}_1^{des}, \ldots, \bar{p}_m^{des}]^T \in \mathbb{R}^m$ as the respective stack vector of relative positions and target relative positions between the pair of communication agents for the edge $(i, j) = e_k \in \mathcal{E}$, where $\bar{p}_k \triangleq p_{ij} = p_i - p_j, \bar{p}_k^{des} \triangleq p_{ij}^{des} = p_i^{des} - p_j^{des}, k = 1, 2, \ldots, m$. It can be then verified that $Lp = D\bar{p}$ and $\bar{p} = D^T p$. In addition, if $\bar{p} = 0$, we have that $Lp = 0$. Similarly, it holds that $Lp^{des} = D\bar{p}^{des}$, $\bar{p}^{des} = D^T p^{des}$.

By stacking (18) and (19), the dynamics of the leader-follower multi-agent system is rewritten as:

$$\Sigma_1 : \dot{p} = -L(p - p^{des}) + Bu, \tag{20}$$

where L is the graph Laplacian and $B = \begin{bmatrix} 0_{n_f \times n_l} \\ I_{n_l} \end{bmatrix}$.

In the sequel, we denote $x = p - p^{des} = [x_1, \ldots, x_n]^T$ as the shifted absolute position vector with respect to p^{des}. Accordingly, $\bar{x} = \bar{p} - \bar{p}^{des} = [\bar{x}_1, \ldots, \bar{x}_m]^T$ is denoted as the shifted relative position vector with respect to $\bar{p}^{des}$.

The objective is to propose a control strategy for the leader-follower multi-agent system (20) such that it can achieve the target formation $\mathcal{F}$ as in (17). Notably, the control strategy is only applied to the leaders. Moreover, we impose transient constraints on the evolution of the relative positions $\bar{p}_i(t)$ between neighboring agents, which are defined by the following prescribed performance bounds

$$\bar{p}_i^{des} - \rho_{\bar{x}_i}(t) < \bar{p}_i(t) < \bar{p}_i^{des} + \rho_{\bar{x}_i}(t), \tag{21}$$

or equivalently, the evolution of the shifted relative position $\bar{x}_i(t)$ should satisfy

$$-\rho_{\bar{x}_i}(t) < \bar{x}_i(t) < \rho_{\bar{x}_i}(t). \tag{22}$$

Here $\rho_{\bar{x}_i}(t), i = 1, 2, \ldots, m$ are the performance functions as introduced in Subsection 3.2, which can be chosen as

$$\rho_{\bar{x}_i}(t) = (\rho_{\bar{x}_{i0}} - \rho_{\bar{x}_{i\infty}})e^{-l_{\bar{x}_i} t} + \rho_{\bar{x}_{i\infty}}. \tag{23}$$

In summary, we aim to design solely the leader controllers such that the entire heterogeneous leader-follower team can attain desired formation while satisfying the transient constraints that are defined by the prescribed performance functions. The control objectives are graphically depicted in Figure. 3.

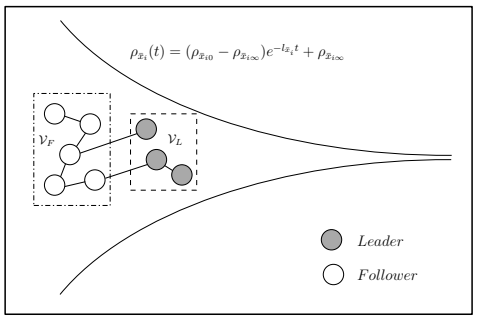

Figure 3: Control objectives for leader-follower multi-agent systems.

4.2. Transient control for first-order leader-follower multi-agent systems

In this subsection, we present a systematic approach for designing only the leader controllers of the first-order heterogeneous leader-follower multi-agent systems (20) to ensure the convergence of the entire team to the desired formation (17) while simultaneously adhering to transient

constraints (21). The discussion in this subsection relies on references [101, 102].

Given that the transient constraints (21) are for the relative positions, we first rewrite the dynamics of the leader-follower multi-agent system (20) into the edge space to characterize the dynamics of the relative positions. The associated incidence matrix is decomposed into the first n_f and the remaining last n_l rows, i.e., $D = \begin{bmatrix} D_F^T & D_L^T \end{bmatrix}^T$ [97] with D_F, D_L denoting the incidence matrices with respect to the followers and leaders, respectively. The dynamics (20) are then reorganized as

$$\Sigma_1 : \begin{bmatrix} \dot{x}_F \\ \dot{x}_L \end{bmatrix} = \begin{bmatrix} A_F & B_F \\ B_F^T & A_L \end{bmatrix} \begin{bmatrix} x_F \\ x_L \end{bmatrix} + \begin{bmatrix} 0_{n_f \times n_l} \\ I_{n_l} \end{bmatrix} u, \tag{24}$$

where $x_F = [x_1, \ldots, x_{n_f}]^T, x_L = [x_{n_f+1}, \ldots, x_n]^T$ and $A_F = D_F D_F^T, B_F = D_F D_L^T, A_L = D_L D_L^T$. The incidence matrix D essentially describes the relationship between the node space and the edge space. Multiplying both sides of (24) by D^T, we derive the dynamics in the edge space given by

$$\Sigma_{e1} : \dot{\bar{x}} = -L_e \bar{x} + D_L^T u, \tag{25}$$

where L_e represents the edge Laplacian. It is noteworthy that L_e is positive definite when the underlying graph is a tree [103]. Therefore, we make an initial assumption that the graph is a tree, which will be relaxed later.

Assumption 1. *The graph $\mathcal{G} = (\mathcal{V}, \mathcal{E})$ is a tree.*

For the edge dynamics (25), the proposed controller applied to the leader agents is the composition of the term based on prescribed performance of the positions of the neighboring agents:

$$u_j = -\sum_{i \in \Phi_j} g_{\bar{x}_i} \mathcal{J}_{T_{\bar{x}_i}}(\hat{\bar{x}}_i, t) \varepsilon_{\bar{x}_i}(\hat{\bar{x}}_i), \qquad j \in \mathcal{V}_L, \tag{26}$$

where $\Phi_j = \{i | (j,k) = i, k \in \mathcal{N}_j\}$, i.e., the set of all the edges that include agent $j \in \mathcal{V}_L$ as a node, and $g_{\bar{x}_i}$ is a positive scalar gain to be appropriately tuned. Therefore, the proposed control (26) is distributed, requiring only local information. The term $\mathcal{J}_{T_{\bar{x}_i}}$, which includes gradient information, dictates the direction of control. On the other hand, $\varepsilon_{\bar{x}_i}$ determines control strength, as it increases as the trajectory approaches the transient bound. Then, the stack input vector is

$$u = -D_L \mathcal{J}_{T_{\hat{\bar{x}}}} G_{\bar{x}} \varepsilon_{\hat{\bar{x}}}, \tag{27}$$

where $\hat{\bar{x}} \in \mathbb{R}^m$ is the stack vector of transformed errors $\hat{\bar{x}}_i$, $G_{\bar{x}} \in \mathbb{R}^{m \times m}$ is the positive definite diagonal gain matrix with entries the positive constant parameters $g_{\bar{x}_i}$, $\mathcal{J}_{T_{\hat{\bar{x}}}} \triangleq \mathcal{J}_T(\hat{\bar{x}}, t) \in \mathbb{R}^{m \times m}$ is a time-varying diagonal matrix with diagonal entries $\mathcal{J}_{T_{\bar{x}_i}}(\hat{\bar{x}}_i, t)$ given in (8), and $\varepsilon_{\hat{\bar{x}}} \triangleq \varepsilon(\hat{\bar{x}}) \in \mathbb{R}^m$ is the stack vector with entries $\varepsilon_{\bar{x}_i}(\hat{\bar{x}}_i)$.

The following theorem presents the result for formation control of leader-follower multi-agent systems under transient constraints.

Theorem 4.1. *[101, 102] Consider the leader-follower multi-agent system Σ_1 under Assumption 1 with dynamics (20), the predefined performance functions $\rho_{\bar{x}_i}$ as in (23) and the transformed functions $T_{\bar{x}_i}(\hat{\bar{x}}_i)$ as in (5) s.t. $T_{\bar{x}_i}(0) = 0$, and assume that the initial conditions $\bar{p}_i(0)$ are within the performance bounds (21). If the following condition holds:*

$$\bar{\gamma} \geq l = \max_{i=1,\ldots,m} (l_{\bar{x}_i}), \tag{28}$$

where l is the largest decay rate of $\rho_{\bar{x}_i}(t)$ and $\bar{\gamma}$ is the maximum value of γ that ensures:

$$\Gamma = \begin{bmatrix} D_L^T D_L & \frac{1}{2}\left(L_e - \gamma\left(I_m - D_L^T D_L\right)\right) \\ \frac{1}{2}\left(L_e - \gamma\left(I_m - D_L^T D_L\right)\right) & \gamma L_e \end{bmatrix} \geq 0, \tag{29}$$

then the controlled system achieves the target formation (17) and satisfies (21) when applying the control law (27).

Theorem 4.1 proposes a sufficient condition and indicates the trade-offs between the largest decay rate of the performance functions and the leader-follower topology. Note that conditions (28) and (29) are not part of the control laws. (29) is determined by the pair of matrices (L_e, D_L) that characterizes the leader-follower graph topology. Based on Theorem 4.1, we can first derive the maximum value $\bar{\gamma}$ of γ that solves (29). Then, the predefined decay rate l cannot exceed $\bar{\gamma}$, which is useful in practical to design the performance functions.

In the following, we will delve into the results pertaining to two specific classes of tree graphs, namely the path graph and the star graph. Initially, we will focus on the path graph—a graph extensively employed in various applications, such as multi-vehicle platooning.

Definition 1. *A path graph $\mathcal{G}^c = (\mathcal{V}^c, \mathcal{E}^c)$ is a tree graph with vertices set $\mathcal{V}^c = \{1, 2, \ldots, n\}, n \geq 2$ and edges set $\mathcal{E}^c = \{(i, i+1) \in \mathcal{V}^c \times \mathcal{V}^c \mid i \in \mathcal{V}^c \setminus \{n\}\}$ indexed by $e_i = (i, i+1), i = 1, 2, \ldots, n-1$.*

Note that (28) in Theorem 4.1 is a sufficient but not necessary condition, which can be conservative based solely on the analysis of matrix properties. In Subsection 4.5, we will directly investigate the leader-follower topology to establish a stronger topological condition.

Proposition 4.2. *[101, 102] Consider the leader-follower multi-agent system Σ_1 described by (20) with the communication path graph $\mathcal{G}^c = (\mathcal{V}^c, \mathcal{E}^c)$ and the followers set $\mathcal{V}_F^c = \{1, 2, \ldots, n_f\}$, the predefined performance functions $\rho_{\bar{x}_i}$ as in (23) and the transformed function $T_{\bar{x}_i}(\hat{\bar{x}}_i)$ as in (5) s.t. $T_{\bar{x}_i}(0) = 0$, and assume that the initial conditions $\bar{p}_i(0)$ are within the performance bounds (21). Then, we have that*

$$\begin{aligned} &\max_{i=1,\ldots,m} (l_{\bar{x}_i}) = l \leq 2, \qquad n_f = 2; \\ &\max_{i=1,\ldots,m} (l_{\bar{x}_i}) = l \leq 1, \qquad n_f = 3, \end{aligned} \tag{30}$$

are the respective conditions on the largest decay rate of the performance functions $\rho_{\bar{x}_i}$ such that the path achieves

the target formation (17) *and satisfies* (21) *when applying* (27).

Now, let us consider another specific class, the star graph $\mathcal{G}^s = (\mathcal{V}^s, \mathcal{E}^s)$, defined as follows.

Definition 2. *A star graph $\mathcal{G}^s = (\mathcal{V}^s, \mathcal{E}^s)$ is a tree graph with vertices set $\mathcal{V}^s = \{1, 2, \ldots, n\}, n \geq 2$ where vertex n is called the centering node, and the edges set $\mathcal{E}^s = \{(i, n) \in \mathcal{V}^s \times \mathcal{V}^s \mid i \in \mathcal{V}^s \setminus \{n\}\}$ indexed by $e_i = (i, n), i = 1, 2, \ldots, n-1$.*

Then, the following result can be obtained based on Theorem 4.1.

Proposition 4.3. *[101, 102] Consider the leader-follower multi-agent system Σ_1 described by* (20) *with the communication star graph $\mathcal{G}^s = (\mathcal{V}^s, \mathcal{E}^s)$ and the leader set $\mathcal{V}_L^s = \{n\}$, the predefined performance functions $\rho_{\bar{x}_i}$ as in* (23) *and the transformed function $T_{\bar{x}_i}(\hat{\bar{x}}_i)$ as in* (5) *s.t. $T_{\bar{x}_i}(0) = 0$, and assume that the initial conditions $\bar{p}_i(0)$ are within the performance bounds* (21)*. If*

$$\max_{i=1,\ldots,m} (l_{\bar{x}_i}) = l \leq 1, \tag{31}$$

then the controlled system achieves the target formation (17) *and satisfies the prescribed performance bounds* (21) *when applying the control law* (27)*.*

4.3. Transient control for second-order leader-follower multi-agent Systems

In this subsection, we explore an extension of second-order heterogeneous leader-follower multi-agent systems. The discussion in this subsection relies on references [104, 102].

let $p_i, v_i \in \mathbb{R}$ be the respective position and velocity of agent i. We also aim to design a control strategy for the second-order leader-follower multi-agent system such that it can achieve the relative position-based formation. The state evolution of each follower $i \in \mathcal{V}_F$ is now governed by the second-order formation protocol:

$$\begin{aligned} \dot{p}_i &= v_i \\ \dot{v}_i &= -\sum_{j \in \mathcal{N}_i} \left((p_i - p_j - p_{ij}^{des}) + (v_i - v_j) \right). \end{aligned} \tag{32}$$

In parallel, the state evolution of each leader $i \in \mathcal{V}_L$ is determined by the second-order formation protocol with an external input $u_i \in \mathbb{R}$:

$$\begin{aligned} \dot{p}_i &= v_i \\ \dot{v}_i &= -\sum_{j \in \mathcal{N}_i} \left((p_i - p_j - p_{ij}^{des}) + (v_i - v_j) \right) + u_i. \end{aligned} \tag{33}$$

We further denote $v = [v_1, \ldots, v_n]^T \in \mathbb{R}^n$ as the stack vector of velocities, and $\bar{v} = [\bar{v}_1, \ldots, \bar{v}_m]^T \in \mathbb{R}^m$ as the stack vector of relative velocities between the pair of communication agents for the edge $(i, j) = k \in \mathcal{E}$, where $\bar{v}_k \triangleq v_{ij} = v_i - v_j, k = 1, 2, \ldots, m$. Similarly, it holds that $Lv = D\bar{v}$, $\bar{v} = D^T v$.

By stacking (32) and (33), the dynamics of the second-order leader-follower multi-agent system is rewritten as:

$$\Sigma_2 : \begin{bmatrix} \dot{p} \\ \dot{v} \end{bmatrix} = \begin{bmatrix} 0_n & I_n \\ -L & -L \end{bmatrix} \begin{bmatrix} p - p^{des} \\ v \end{bmatrix} + \begin{bmatrix} 0_{n \times n_l} \\ B \end{bmatrix} u, \tag{34}$$

where L is the graph Laplacian and $B = \begin{bmatrix} 0_{n_f \times n_l} \\ I_{n_l} \end{bmatrix}$.

Our target for the second-order case is still to design a control strategy for the leader-follower multi-agent system (34) such that it can achieve the target formation $\mathcal{F}$ as in (17) while satisfying the transient constraints (21) or (22). Similar to the first-order case, we first rewrite the dynamics of the second-order leader-follower multi-agent system (34) into the edge space as

$$\Sigma_{e2} : \begin{bmatrix} \dot{\bar{x}} \\ \dot{\bar{v}} \end{bmatrix} = \begin{bmatrix} 0_m & I_m \\ -L_e & -L_e \end{bmatrix} \begin{bmatrix} \bar{x} \\ \bar{v} \end{bmatrix} + \begin{bmatrix} 0_{m \times n_l} \\ D_L^T \end{bmatrix} u. \tag{35}$$

For (35), we first design the reference velocity $v_d \in \mathbb{R}^n$ and the corresponding reference relative velocity $\bar{v}_d \in \mathbb{R}^m$ as:

$$v_d = -D\mathcal{J}_{T_{\hat{\bar{x}}}} G_{\bar{x}} \varepsilon_{\hat{\bar{x}}}; \qquad \bar{v}_d = -L_e \mathcal{J}_{T_{\hat{\bar{x}}}} G_{\bar{x}} \varepsilon_{\hat{\bar{x}}}, \tag{36}$$

where the parameters are similar to those defined in (27). We then define the relative velocity error vector as $\bar{e} = [\bar{e}_1, \ldots, \bar{e}_m]^T = \bar{v} - \bar{v}_d \in \mathbb{R}^m$.

The insights here are basically resorting to first designing the reference relative velocity that can be proven to guarantee the prescribed performance for the relative positions. Then, by defining the relative velocity error, another PPC law with respect to the relative velocities is designed to stabilize the relative velocity error also within certain prescribed performance bounds. Therefore, we also establish the corresponding prescribed performance functions $\rho_{\bar{e}_i}(t)$, the transformation functions $T_{\bar{e}_i}(\hat{\bar{e}}_i)$, and the transformed error $\varepsilon_{\bar{e}_i}(\hat{\bar{e}}_i)$ for the relative velocity errors, $i = 1, 2, \ldots, m$. These terms exhibit similarities to those defined for the shifted relative positions. The corresponding prescribed performance functions $\rho_{\bar{e}_i}(t)$ related to the relative velocity errors are defined as follows, which are designed in a way such that the initial condition of $\bar{e}_i$ is within the performance bound

$$\rho_{\bar{e}_i}(t) = (\rho_{\bar{e}_{i0}} - \rho_{\bar{e}_{i\infty}}) e^{-l_{\bar{e}_i} t} + \rho_{\bar{e}_{i\infty}}. \tag{37}$$

The related prescribed performance region is described as

$$-\rho_{\bar{e}_i}(t) < \bar{e}_i(t) < \rho_{\bar{e}_i}(t). \tag{38}$$

We then define in a similar manner the normalized error $\bar{e}_i(t)$, the transformation function $T_{\bar{e}_i}$ as

$$T_{\bar{e}_i}(\hat{\bar{e}}_i) = \ln \left(\frac{1 + \hat{\bar{e}}_i}{1 - \hat{\bar{e}}_i} \right), \tag{39}$$

and the transformed error $\varepsilon_{\bar{e}_i}$. Similar to (7), we can derive the normalized Jacobian $\mathcal{J}_{T_{\bar{e}_i}}(\hat{\bar{e}}_i, t)$ of the transformation

function $T_{\bar{e}_i}$ and the normalized derivative $\alpha_{\bar{e}_i}(t)$ of the performance function, respectively.

For the leader-follower multi-agent system (35), the proposed controller applied to each leader agent is the composition of the term based on the prescribed performance of the relative velocity errors of the neighboring agents:

$$u_j = -\sum_{i\in\Phi_j} g_{\bar{e}_i}\mathcal{J}_{T_{\bar{e}_i}}(\hat{\bar{e}}_i,t)\varepsilon_{\bar{e}_i}(\hat{\bar{e}}_i), \quad j\in\mathcal{V}_L, \tag{40}$$

where $\Phi_j = \{i|(j,k)=i, k\in\mathcal{N}_j\}$, i.e., the set of all the edges that include agent $j\in\mathcal{V}_L$ as a node. Then the stack input vector is

$$u = -D_L\mathcal{J}_{T_{\hat{\bar{e}}}}G_{\bar{e}}\varepsilon_{\hat{\bar{e}}}, \tag{41}$$

where the parameters are defined similarly by stacking the parameters in (40).

The following theorem is proposed for second-order leader-follower multi-agent systems such that the prescribed performance can be guaranteed for both relative positions and relative velocity errors. In addition, the target formation (17) can be achieved.

Theorem 4.4. *[104, 102] Consider the leader-follower multi-agent system Σ_2 under Assumption 1 with dynamics* (34)*, and the predefined performance functions $\rho_{\bar{x}_i}$ and $\rho_{\bar{e}_i}$ as in* (23) *and* (37)*, respectively. Suppose the transformation functions $T_{\bar{x}_i}(\hat{\bar{x}}_i)$, $T_{\bar{e}_i}(\hat{\bar{e}}_i)$ are chosen as in* (5)*,* (39) *respectively satisfying $T_{\bar{x}_i}(0)=0, T_{\bar{e}_i}(0)=0$, and assume that the initial conditions $\bar{x}_i(0)$ and $\bar{e}_i(0)$ are within the performance bounds* (21) *and* (38)*, respectively. If the following condition holds:*

$$\bar{\gamma} \geq l' = \max_{i=1,\ldots,m}(l_{\bar{e}_i}), \tag{42}$$

where l' is the largest decay rate of $\rho_{\bar{e}_i}(t)$ and $\bar{\gamma}$ is the maximum value of γ that ensures:

$$\Gamma = \begin{bmatrix} D_L^T D_L & \frac{1}{2}\big(L_e - \gamma\big(I_m - D_L^T D_L\big)\big) \\ \frac{1}{2}\big(L_e - \gamma\big(I_m - D_L^T D_L\big)\big) & \gamma L_e \end{bmatrix} \geq 0, \tag{43}$$

then, the shifted relative position $\bar{x}$ under the control (41) *converges to an arbitrary small ball around zero while satisfying* (22)*. In addition, the relative velocity errors satisfy* (38)*.*

The convergence result of $\bar{x}(t)$ in Theorem 4.4 is practical convergence, which is reasonable in practical design, as demonstrated in [105].

4.4. Leader-follower multi-agent systems with cycles

In this subsection, we focus on distributed formation control for heterogeneous leader-follower multi-agent systems with prescribed transient behavior under general communication graphs that contain cycles to avoid Assumption 1. We also explore the roles of cycles in realizing convergence benefits within the leader-follower framework. The inclusion of cycles showcases more practical significance and provides a complete theory for undirected graphs. The difficulty posed by cycles lies in the inability to directly leverage the positive definiteness of the edge Laplacian for convergence analysis. It becomes necessary to partition the graph into a spanning tree and the additional edges that complete the cycles. The discussion in this subsection relies on reference [106].

We now consider general graphs that contain cycles, i.e., without Assumption 1. We aim to design a control strategy for the first-order leader-follower multi-agent system (20) such that it can achieve the target formation $\mathcal{F}$ as in (17) while satisfying the transient constraints (21) or (22).

Similarly, we need to rewrite (20) into the dynamics corresponding to followers and leaders, respectively. In addition, since we consider a general graph with circles that can be regarded as the union of two edge-disjoint subgraphs on the same vertex set as $\mathcal{G} = \mathcal{G}_t \cup \mathcal{G}_c$, where $\mathcal{G}_t$ is a spanning tree subgraph and $\mathcal{G}_c$ contains the remaining edges that complete the cycles in $\mathcal{G}$ [107]. The corresponding incidence matrix is decomposed as

$$D = \begin{bmatrix} D_F^t & D_F^c \\ D_L^t & D_L^c \end{bmatrix}, D^t = \begin{bmatrix} D_F^t \\ D_L^t \end{bmatrix}, D^c = \begin{bmatrix} D_F^c \\ D_L^c \end{bmatrix}, \tag{44}$$

and $D_F = \begin{bmatrix} D_F^t & D_F^c \end{bmatrix}$, $D_L = \begin{bmatrix} D_L^t & D_L^c \end{bmatrix}$ with $D_F^t \in \mathbb{R}^{n_f\times(n-1)}, D_F^c \in \mathbb{R}^{n_f\times(m-n+1)}$, $D_L^t \in \mathbb{R}^{n_l\times(n-1)}, D_L^c \in \mathbb{R}^{n_l\times(m-n+1)}$. In essence, the incidence matrix D is partitioned by rows into the first n_f rows and the remaining last n_l rows, denoted as $D = \begin{bmatrix} D_F^T & D_L^T \end{bmatrix}^T$ [97]. Additionally, the matrix is decomposed by columns into the first $n-1$ columns and the remaining last $m-n+1$ columns, given by $D = \begin{bmatrix} D^t & D^c \end{bmatrix}$ with D^t, D^c denoting the edges of the spanning tree subgraph $\mathcal{G}_t$ and the remaining edges of $\mathcal{G}_c$ that complete the cycles in $\mathcal{G}$, respectively. Then, the dynamics (20) are reorganized into the edge space as

$$\Sigma_e : \dot{\bar{x}} = -L_e\bar{x} + D_L^T u, \tag{45}$$

with L_e being the edge Laplacian which is positive definite if the graph is a tree [103]. Hence, we have that the edge Laplacian $L_e^t = {D^t}^T D^t$ for the spanning tree subgraph $\mathcal{G}_t$ is positive definite. For a general graph with cycles, the edge Laplacian L_e in (45) is only positive semidefinite, but it can be represented by the edge Laplacian L_e^t of its spanning tree $\mathcal{G}_t$ according to [107]. Specifically, the columns of D^c are linearly dependent on the columns of D^t, which can be expressed as $D^c = D^t T$ with $T = ({D^t}^T D^t)^{-1}{D^t}^T D^c = (L_e^t)^{-1}{D^t}^T D^c$. Then, we have that $D = \begin{bmatrix} D^t & D^c \end{bmatrix} = \begin{bmatrix} D^t & D^t T \end{bmatrix} = D^t \begin{bmatrix} I_{n-1} & T \end{bmatrix}$. We further denote the transformation matrix R as

$$R = \begin{bmatrix} I_{n-1} & T \end{bmatrix}. \tag{46}$$

Thus $D = D^t R$ and the relation between L_e and L_e^t is derived as $L_e = R^T L_e^t R$.

For the edge dynamics (45), the controller applied to the leader agents is proposed as follows:

$$u_j = -\sum_{i\in\Phi_j} g_{\bar{x}_i}\mathcal{J}_{T_{\bar{x}_i}}(\hat{\bar{x}}_i,t)\varepsilon_{\bar{x}_i}(\hat{\bar{x}}_i), \quad j\in\mathcal{V}_L, \tag{47}$$

where $\Phi_j = \{i|(j,k) = i, k \in \mathcal{N}_j\}$, and the stack input vector is

$$u = -D_L \mathcal{J}_{T_{\hat{\tilde{x}}}} G_{\bar{x}} \varepsilon_{\hat{\tilde{x}}}, \tag{48}$$

which is similar to (27). The difference here is that we now take the cycles into account.

We now develop the following result for transient control of leader-follower multi-agent systems under general communication graphs with cycles.

Theorem 4.5. *[106] Consider the leader-follower multi-agent system Σ with dynamics (20), the predefined performance functions $\rho_{\bar{x}_i}$ as in (23) and the transformed functions $T_{\bar{x}_i}(\hat{\tilde{x}}_i)$ as in (5) s.t. $T_{\bar{x}_i}(0) = 0$, and assume that the initial conditions $\bar{p}_i(0)$ are within the performance bounds (21). If the following condition holds:*

$$\bar{\gamma} \geq l = \max_{i=1,\ldots,m}(l_{\bar{x}_i}), \tag{49}$$

where l is the largest decay rate of $\rho_{\bar{x}_i}(t)$ and $\bar{\gamma}$ is the maximum value of γ that ensures the following block matrix denoted as Γ satisfies $\Gamma \geq 0$:

$$\begin{bmatrix} {D_L^t}^T D_L^t & \frac{1}{2}\big(L_e^t - \gamma\big((RR^T)^{-1} - {D_L^t}^T D_L^t\big)\big) \\ \frac{1}{2}\big(L_e^t - \gamma\big((RR^T)^{-1} - {D_L^t}^T D_L^t\big)\big) & \gamma L_e^t \end{bmatrix}. \tag{50}$$

Then the controlled system achieves the target formation (17) and satisfies (21) when applying the control law (48).

The result in this subsection also indicates the trade-offs between the largest decay rate of the performance functions (23) and the leader amount and positions. Theorem 4.5 also indicates how the cycles in a graph will benefit the convergence result.

4.5. Topological conditions for enabling transient control in leader-follower networks

In this subsection, we address the challenge of establishing both necessary and sufficient conditions for leader-follower multi-agent systems to attain the desired relative position-based formation while adhering to specified performance guarantees. The analysis covers general graphs that include cycles. We first investigate the necessary conditions for the leader-follower graph topology. Subsequently, these necessary conditions are extended to both the necessary and sufficient conditions for leader-follower formation control with prescribed performance. The main motivation stems from the fact that the results discussed in the previous subsections are only sufficient. There exist leader-follower multi-agent systems for which, irrespective of the control design made for the leaders, the transient bounds can be always violated. This may occur, for instance, when an insufficient number of leaders are chosen or when leaders are assigned unsuitable positions. Hence, our objective in this subsection is to explore stronger topological conditions on leader-follower graph topology such that we can design the leader controllers to steer the entire system to achieve the target formation while fulfilling the prescribed performance behavior. The discussion in this subsection relies on reference [108].

We initially establish necessary conditions on the graph topology for both tree graphs and general graphs with cycles. Specifically, we first define a *leaderless graph* $\mathcal{G}^f = (\mathcal{V}^f, \mathcal{E}^f)$ with only followers, i.e., $\mathcal{V}_F^f = \mathcal{V}^f$, $\mathcal{V}_L^f = \emptyset$ and $\mathcal{E}_{FF}^f = \mathcal{E}^f$. The definitions of a subgraph and an induced subgraph are detailed below:

Definition 3. *(Subgraph and induced subgraph.) A graph $\mathcal{G}' = (\mathcal{V}', \mathcal{E}')$ is a subgraph of the graph $\mathcal{G} = (\mathcal{V}, \mathcal{E})$, if the following conditions hold:*

- *$\mathcal{V}' \subseteq \mathcal{V}$ and $\mathcal{E}' \subseteq \mathcal{E}$;*
- *for any $i \in \mathcal{V}_F'$ we have $i \in \mathcal{V}_F$ and for any $i \in \mathcal{V}_L'$ we have $i \in \mathcal{V}_L$.*

A subgraph $\mathcal{G}'$ of $\mathcal{G}$ is an induced subgraph of $\mathcal{G}$, denoted as $\mathcal{G}' \subseteq \mathcal{G}$ if it further holds that for any edge $(i,j) \in \mathcal{E}, i,j \in \mathcal{V}'$, we have $(i,j) \in \mathcal{E}'$.

We can then define a path in a graph $\mathcal{G}$ as a subgraph of $\mathcal{G}$.

Definition 4. *(Path subgraph.) A path p of the graph $\mathcal{G} = (\mathcal{V}, \mathcal{E})$ is called a path subgraph $p = (\mathcal{V}^p, \mathcal{E}^p)$ of $\mathcal{G}$ such that the following conditions hold:*

- *$\mathcal{V}^p \subseteq \mathcal{V}$ and $\mathcal{E}^p \subseteq \mathcal{E}$;*
- *for any $i \in \mathcal{V}_F^p$ we have $i \in \mathcal{V}_F$ and for any $i \in \mathcal{V}_L^p$ we have $i \in \mathcal{V}_L$.*

Denote each column (corresponding to an edge) of the incidence matrix of $\mathcal{G}^f$ by the vector e_i. Then $(L_e)_{ij} = e_i^T e_j = c_{ij} = 2$ if $i = j$; $c_{ij} = 0$ if e_i, e_j share no nodes; $c_{ij} = \pm 1$ if e_i, e_j share a single node [107]. Based on these simple rules, we can define the neighbors of edge e_i as $\mathcal{N}(e_i) := \{e_j \mid |e_i^T e_j| = 1\}$. Then the following lemma is proposed for tree graphs and acts as a basis for the later extended results for general graphs with cycles.

Lemma 4.6. *[108] Consider the leader-follower multi-agent system (20) described by the tree graph $\mathcal{G} = (\mathcal{V}, \mathcal{E})$. A necessary condition on $\mathcal{G}$ under which we can design the leaders using (48) to achieve the target formation $\mathcal{F}$ as in (17) while satisfying (21) is that every leaderless graph $\mathcal{G}^f = (\mathcal{V}^f, \mathcal{E}^f)$, such that $\mathcal{G}^f \subseteq \mathcal{G}$, should satisfy*

$$|\mathcal{N}(e_i)| \leq 2, \quad \forall e_i \in \mathcal{E}^f. \tag{51}$$

For graph with cycles, we first denote $\mathcal{E}(\mathcal{C})$ as the edge set of the cycle $\mathcal{C}$ with cardinality $|\mathcal{E}(\mathcal{C})|$. We then execute the graph decomposition procedure, which we refer to as *complete decomposition*.

Definition 5. *(Complete decomposition.) A graph $\mathcal{G} = (\mathcal{V}, \mathcal{E})$ is decomposed with respect to the edge $e_i \in \mathcal{E}$ as $\mathcal{G} := \cup_{\mathcal{C}_{e_i} \in \mathcal{X}_i} \mathcal{C}_{e_i} \cup \mathcal{P}_i$, where $\mathcal{X}_i := \{\mathcal{C}_{e_i} \mid e_i \in \mathcal{C}_{e_i}\}$ is the cycle set composed of all the cycles $\mathcal{C}_{e_i}$ in $\mathcal{G}$ that contain e_i as an edge, and satisfy:*

– *for every pair* $\mathcal{C}^a_{e_i}, \mathcal{C}^b_{e_i} \in \mathcal{X}_i$, $(\mathcal{N}(e_i) \cap \mathcal{C}^a_{e_i}) \cap (\mathcal{N}(e_i) \cap \mathcal{C}^b_{e_i}) = \emptyset$.

– *for every* $\mathcal{C}_{e_i} \in \mathcal{X}_i$, *there does not exist a cycle* $\mathcal{C}$ *of* $\mathcal{G}$ *such that* $e_i \in \mathcal{C}$, $(\mathcal{N}(e_i) \cap \mathcal{C}_{e_i}) \cap (\mathcal{N}(e_i) \cap \mathcal{C}) \neq \emptyset$, *and* $|\mathcal{E}(\mathcal{C})| < |\mathcal{E}(\mathcal{C}_{e_i})|$,

and where $\mathcal{P}_i := \{e_k \mid e_k \notin \mathcal{C}_{e_i}, \mathcal{C}_{e_i} \in \mathcal{X}_i\}$ *is the set of the edges that do not belong to any cycle in* $\mathcal{X}_i$. *Then, we call this decomposition a complete decomposition of* $\mathcal{G}$ *with respect to the edge* $e_i \in \mathcal{E}$.

Next, we elucidate the complete decomposition with the following example.

Example 4.7. *Consider two leaderless graphs as shown in Figure.4. In the left figure, the complete decomposition with respect to the edge* e_1 *is* $\mathcal{G} := \cup_{\mathcal{C}_{e_1} \in \mathcal{X}_1} \mathcal{C}_{e_1} \cup \mathcal{P}_1$, *where the cycle set* $\mathcal{X}_1$ *includes only the cycle on the top, i.e., the cycle composed by the edges* e_1, e_2, e_3, *and* $\mathcal{P}_1 = \{e_4, e_5, e_6\}$. *The complete decomposition with respect to the edge* e_3 *is* $\mathcal{G} := \cup_{\mathcal{C}_{e_3} \in \mathcal{X}_3} \mathcal{C}_{e_3} \cup \mathcal{P}_3$, *where the cycle set* $\mathcal{X}_3$ *includes the cycle composed by the edges* e_1, e_2, e_3 *and the cycle composed by the edges* e_3, e_4, e_5, e_6, *and thus* $\mathcal{P}_3 = \emptyset$. *In the right figure, the complete decomposition with respect to the edge* e_4 *is* $\mathcal{G} := \cup_{\mathcal{C}_{e_4} \in \mathcal{X}_4} \mathcal{C}_{e_4} \cup \mathcal{P}_4$, *where the cycle set* $\mathcal{X}_4$ *includes the cycle composed by the edges* e_1, e_4, e_5 *and the cycle composed by the edges* e_3, e_4, e_6; $\mathcal{P}_4 = \{e_2, e_7\}$ *and thus* $\mathcal{N}(e_4) \cap \mathcal{P}_4 = \{e_7\}$.

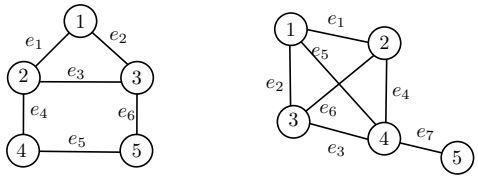

Figure 4: Complete decomposition examples.

The complete decomposition decomposes a large scale graph into certain cycles along with the remaining edges that do not belong to any cycle. We can then derive the necessary condition for $\mathcal{G}$ based on the decomposed cycle set $\mathcal{X}_i$ with respect to the edge $e_i \in \mathcal{E}$ and the remaining edges in $\mathcal{P}_i$. The following theorem proposes a necessary condition on general graphs with cycles, under which we can design the leader controllers to achieve the target formation without violating the prescribed performance bounds.

Theorem 4.8. *[108] Consider the leader-follower multi-agent system* (20) *described by the graph* $\mathcal{G} = (\mathcal{V}, \mathcal{E})$. *A necessary condition on* $\mathcal{G}$ *under which we can design the leaders using* (48) *to achieve the target formation* $\mathcal{F}$ *as in* (17) *while satisfying* (21) *is that every leaderless graph* $\mathcal{G}^f = (\mathcal{V}^f, \mathcal{E}^f)$, *such that* $\mathcal{G}^f \subseteq \mathcal{G}$, *should satisfy*

$$\sum_{\mathcal{C}_{e_i} \in \mathcal{X}_i} \{\min(|\mathcal{E}(\mathcal{C}_{e_i})| - 4, 2)\} + |E_i| \leq 2, \quad \forall e_i \in \mathcal{E}^f. \quad (52)$$

where $E_i = \{e_k \mid e_k \in \mathcal{N}(e_i) \cap \mathcal{P}_i\}$, *and* $\mathcal{X}_i$ *is the cycle set obtained via the complete decomposition of* $\mathcal{G}^f$ *with respect to* e_i *as in Definition 5.*

Based on Lemma 4.6 and Theorem 4.8, we proceed to establish sufficient conditions on the graph topology applicable to both tree graphs and general graphs with cycles. It is essential to emphasize that the conditions outlined in Lemma 4.6 and Theorem 4.8 are necessary but not sufficient since we only check the induced subgraphs (as in Definition 3) comprising only followers. The conditions specified in Lemma 4.6 or Theorem 4.8 lack sufficiency when considering the presence and impact of leader vertices.

In the sequel, we take the choice of leader vertices into account and focus on finding a sufficient condition on the graph topology, which leads to a necessary and sufficient condition. We first define the following follower-leader-follower (FLF) path and maximum follower-end subgraph as

Definition 6. *(FLF path.) A path subgraph* $p = (\mathcal{V}^p, \mathcal{E}^p) \in P$ *of* $\mathcal{G} = (\mathcal{V}, \mathcal{E})$ *as in Definition 4 with* $v_i, v_j \in \mathcal{V}^p$ *as the two end nodes, is a FLF path of* $\mathcal{G}$ *if* $\mathcal{V}^p_F = \{v_i, v_j\}$. P *is the collection of all the FLF paths of* $\mathcal{G}$. *The neighborhood of the FLF path* $p \in P$ *denoted as* $\mathfrak{N}(p)$ *is the set of edges that share the node* v_i *or* v_j *with* p, *i.e.,* $\mathfrak{N}(p) = \{e_k \mid v_i \in \mathbf{v}(e_k)$ *or* $v_j \in \mathbf{v}(e_k), e_k \in \mathcal{E} \setminus \mathcal{E}^p\}$.

Definition 7. *(Maximum follower-end subgraph.) A graph* $\mathcal{G}^\star = (\mathcal{V}^\star, \mathcal{E}^\star)$ *is a maximum follower-end subgraph of the graph* $\mathcal{G} = (\mathcal{V}, \mathcal{E})$, *denoted as* $\mathcal{G}^\star \preceq \mathcal{G}$ *if the following conditions hold:*

– $\mathcal{G}^\star \subseteq \mathcal{G}$ *(as in Definition 3);*

– *every* $i \in \mathcal{V}^\star_L$ *belongs to a FLF path of* $\mathcal{G}^\star$*;*

– *there is no subgraph* $\mathcal{G}' = (\mathcal{V}', \mathcal{E}')$ *of* $\mathcal{G}$ *such that every* $i \in \mathcal{V}'_L$ *belongs to a FLF path satisfying* $|\mathcal{V}'| > |\mathcal{V}^\star|$.

Definition 7 aims to generate an induced subgraph $\mathcal{G}^\star$ of $\mathcal{G}$ that ignores the end leaders as they have the freedom to move while maximizing the inclusion of agents. Since the collection of all FLF paths P traverses all the edges $e_i \in \mathcal{E}^\star_{LF} \cup \mathcal{E}^\star_{LL}$, the subsequent discussion focuses on the convergence results for FLF paths. When considering the maximum follower-end subgragh $\mathcal{G}^\star$, we can also completely decompose $\mathcal{G}^\star$ with respect to a specific FLF path $p_i \in P$. The complete decomposition of a graph $\mathcal{G}$ in relation to a particular FLF path p_i is defined similarly to Definition 5.

Definition 8. *(Complete decomposition w.r.t. FLF path.) A graph* $\mathcal{G} = (\mathcal{V}, \mathcal{E})$ *is decomposed with respect to the FLF path* $p_i \in P$ *as* $\mathcal{G} := \cup_{\mathcal{C}_{p_i} \in \mathcal{Y}_i} \mathcal{C}_{p_i} \cup \mathcal{Q}_i$, *where* $\mathcal{Y}_i := \{\mathcal{C}_{p_i} \mid p_i \subseteq \mathcal{C}_{p_i}\}$ *is the cycle set composed of all the cycles* $\mathcal{C}_{p_i}$ *in* $\mathcal{G}$ *that contain* p_i *as per Definition 4 and satisfy:*

– *for every pair of* $\mathcal{C}^a_{p_i}, \mathcal{C}^b_{p_i} \in \mathcal{Y}_i$, $(\mathfrak{N}(p_i) \cap \mathcal{C}^a_{p_i}) \cap (\mathfrak{N}(p_i) \cap \mathcal{C}^b_{p_i}) = \emptyset$.

– *for every $\mathcal{C}_{p_i} \in \mathcal{Y}_i$, there does not exist a cycle $\mathcal{C}$ of $\mathcal{G}$ such that $p_i \subseteq \mathcal{C}, (\mathfrak{N}(p_i) \cap \mathcal{C}_{p_i}) \cap (\mathfrak{N}(p_i) \cap \mathcal{C}) \neq \emptyset$, and $|\mathcal{E}(\mathcal{C})| < |\mathcal{E}(\mathcal{C}_{p_i})|$,*

and where $\mathcal{Q}_i := \{e_k \mid e_k \notin \mathcal{C}_{p_i}, \mathcal{C}_{p_i} \in \mathcal{Y}_i\}$ is the set of the edges that do not belong to any cycle in $\mathcal{Y}_i$. Then, we call this decomposition a complete decomposition of $\mathcal{G}$ with respect to the FLF path $p_i \in P$.

We now establish the following theorem outlining the necessary and sufficient graph topological conditions for the leader-follower multi-agent system to attain the target formation $\mathcal{F}$ as defined in (17) while satisfying the prescribed performance bounds (21).

Theorem 4.9. *[108] Consider the leader-follower multi-agent system (20) described by the graph $\mathcal{G} = (\mathcal{V}, \mathcal{E})$, and let $\mathcal{G}^\star \preceq \mathcal{G}$. A necessary and sufficient condition on $\mathcal{G}$ under which we can design the leaders using (48) to achieve the target formation $\mathcal{F}$ as in (17) while satisfying (21) is that:*

– *for any $e_i \in \mathcal{E}^\star_{FF}$,*

$$\sum_{\mathcal{C}_{e_i} \in \mathcal{X}_i} \{\min(|\mathcal{E}(\mathcal{C}_{e_i})| - 4, 2)\} + |E_i| \leq 2; \tag{53}$$

– *for any $p_i \in P^\star$, there either exists $\mathcal{C}_{p_i} \in \mathcal{Y}_i$ such that $|\mathcal{E}(\mathcal{C}_{p_i})| < 2|\mathcal{E}(p_i)|$, or*

$$\sum_{\mathcal{C}_{p_i} \in \mathcal{Y}_i} \{\min(|\mathcal{E}(\mathcal{C}_{p_i})| - 2|\mathcal{E}(p_i)| - 2, 2)\} + |F_i| \leq 2, \tag{54}$$

where $E_i = \{e_k \mid e_k \in \mathcal{N}(e_i) \cap \mathcal{P}_i\}$, $\mathcal{X}_i$ is the cycle set obtained via the complete decomposition of $\mathcal{G}^\star$ with respect to $e_i \in \mathcal{E}^\star_{FF}$ as in Definition 5, $P^\star$ is the collection of all FLF paths of $\mathcal{G}^\star$, $F_i = \{e_k \mid e_k \in \mathfrak{N}(p_i) \cap \mathcal{Q}_i\}$, and $\mathcal{Y}_i$ is the cycle set obtained via the complete decomposition of $\mathcal{G}^\star$ with respect to $p_i \in P^\star$ as in Definition 8.

Theorem 4.9 presents a necessary and sufficient condition regarding the leader-follower graph topology, which enables the design of only the leader controllers in such a way that the entire system can be steered to achieve the target formation within the transient constraints. Moreover, it presents a methodology to tackle leader selection problems amidst transient constraints. Additionally, it offers insights into studying the network's resilience in terms of agent failures and exploring network reconfigurations.

In the end, we present a simple example of multi-vehicle platooning to provide more insights for the theoretical results discussed in Section 4. For a diverse range of simulation scenarios involving various dynamics, topologies, and leader selections, we direct readers to [102, 108].

Example 4.10. ***Multi-vehicle platooning:*** *consider a platoon of 9 vehicles as shown in Figure. 5 with $\mathcal{V}_L = \{v_3, v_4, v_7, v_9\}$. All edges are subject to (21) with $\rho_{\bar{x}_i}(t) = 20e^{-t} + 0.1$ and $\bar{p}_i^{des} = 30$. The transient constraints under consideration encapsulate two primary tasks: ensuring collision avoidance with a minimum distance of 10 and maintaining connectivity within a maximum distance of 50. Additionally, these constraints impose requirements on transient behavior, particularly regarding convergence rate and overshoot towards the target platoon formation. We can observe that the conditions outlined in Theorem 4.9 are trivially met for multi-vehicle platooning, as each vehicle has at most 2 neighboring vehicles. Simulation results obtained by implementing the PPC strategy (48) are depicted in Figure 6. The top plot illustrates platoon evolutions (dashed curves) within the reference frame of the end vehicle (indexed by 9). The initial platoon is represented in black, while the final platoon, achieving a distance of 30 between neighboring vehicles, is depicted in blue. It can be verified that all trajectories of relative positions between neighboring vehicles evolve within the transient performance bounds, as shown in the bottom plot.*

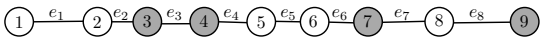

Figure 5: Path graph for multi-vehicle platooning.

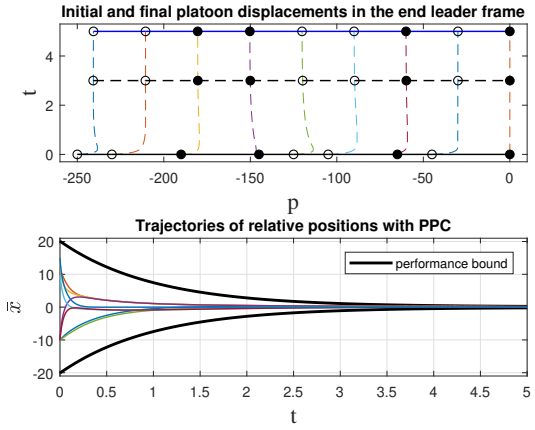

Figure 6: Platoon displacements (top) and trajectories of relative positions (bottom).

5. Cooperative control under spatiotemporal constraints

In the previous section, we have mainly focused on the low-level transient control for the heterogeneous leader-follower multi-agent systems, where the transient constraints are imposed on the whole team but the freedom for control design is only assigned to the leaders. Furthermore, we explore the topological conditions within heterogeneous leader-follower networks such that the target objective can be attained while adhering to the specified transient constraints. In this section, we consider cooperative control and planning of heterogeneous multi-agent

systems under spatiotemporal logic tasks. It is noteworthy that the leader-follower multi-agent systems discussed in the preceding section can be regarded as a subset within the broader category of heterogeneous multi-agent systems. Such complex and high-level tasks are represented by STL specifications, which characterize both time and space constraints.

5.1. Funnel control for heterogeneous leader-follower systems under global STL specifications

In this subsection, we consider leader-follower multi-agent systems subject to a global signal temporal logic specification. Firstly, we present a control strategy based on funnels designed for leader-follower multi-agent systems. This strategy aims to ensure the fulfillment of basic STL formulas by prescribing certain transient behavior within the funnels, which impose constraints on the closed-loop trajectories. Subsequently, a hybrid control strategy is employed to ensure the fulfillment of the sequential STL formulas. The discussion in this subsection relies on reference [109].

Let $x_F = [x_1, \ldots, x_{N_f}]^T \in \mathbb{R}^{nN_f}$ and $x_L = [x_{N_f+1}, \ldots, x_N]^T \in \mathbb{R}^{nN_l}$ represent the stacked state vectors of all follower and leader agents, respective. Denote $x = [x_F^T, x_L^T]^T \in \mathbb{R}^{nN}$. Let $u = [u_{N_f+1}, \ldots, u_N]^T \in \mathbb{R}^{nN_l}$ be the control input vector. We consider the following dynamics of the leader-follower multi-agent system:

$$\Sigma : \dot{x} = -(L \otimes I_n)x + (B \otimes I_n)u, \tag{55}$$

where $\otimes$ represents Kronecker product for high dimension and $B = \begin{bmatrix} 0_{N_f \times N_l} \\ I_{N_l} \end{bmatrix}$.

We then consider a fragment of the STL introduced in Subsection 3.3, which is defined as follows:

$$\psi := \top \mid \mu \mid \neg\mu \mid \psi_1 \wedge \psi_2 \tag{56a}$$
$$\phi := \mathrm{F}_{[a,b]}\psi \mid \mathrm{G}_{[a,b]}\psi \tag{56b}$$
$$\phi' := \bigwedge_{i=1}^{M} \phi_i \tag{56c}$$

where ψ in (56b) and ψ_1, ψ_2 in (56a) are non-temporal formulas of class ψ as in (56a), and where $\phi_i, i \in \{1, \cdots, M\}$ in (56c) are temporal formulas of class ϕ as in (56b) with time intervals $[a_i, b_i]$ satisfying $b_i \leq a_{i+1}, \forall i \in \{1, \cdots, M-1\}$. The STL fragments as in (56b) and (56c) are sufficiently expressive to address tasks such as formation control, collision avoidance, and connectivity maintenance.

The non-smooth robust semantics $\varrho^{\phi_1 \wedge \phi_2}(x,t)$ can be replaced by a smooth approximation given by $\varrho^{\phi_1 \wedge \phi_2}(x,t) \approx -\frac{1}{\eta}\ln(\sum_{i=1}^{2}\exp(-\eta\varrho^{\phi_i}(x,t)))$, where $\eta > 0$ determines the accuracy of the approximation (more accurate with a larger η). Regardless of the chosen value for η, this smooth approximation is an under approximation. As a result, we can infer that $(x,t) \models \phi_1 \wedge \phi_2$ as long as $-\frac{1}{\eta}\ln(\sum_{i=1}^{2}\exp(-\eta\varrho^{\phi_i}(x,t))) > 0$. The objective is then to develop a control strategy only for the leaders, ensuring that the heterogeneous leader-follower multi-agent system described by (55) can achieve the specified task represented by a STL formula.

We begin by demonstrating the synthesis of a control strategy u for temporal formulas ϕ as defined in (56b). This synthesis utilizes prescribed performance control to ensure that $\varrho^{\phi}(x,0) > 0$, where $x : [0,\infty) \to \mathbb{R}^{nN}$ is the closed-loop solution of (55). PPC employs a funnel-based approach to prescribe the transient behavior within a predefined region, which can be elucidated as follows according to our problem in hand:

$$-\rho(t) + \varrho^{\star} < \varrho^{\psi}(x,0) < \varrho^{\star}. \tag{57}$$

Here, ψ represents the corresponding non-temporal formula within the F and G operators, as illustrated in (56b). This, in conjunction with the temporal operators F and G, constitutes the temporal formulas belonging to the class ϕ. We aim to ensure $\varrho^{\phi}(x,0) > 0$ by prescribing a temporal behavior to the corresponding $\varrho^{\psi}(x,0)$ by appropriately designing the parameters $\rho(t)$ and the positive scalar $\varrho^{\star}$. We define the performance function as $\rho(t) := (\rho_0 - \rho_\infty)e^{-lt} + \rho_\infty$, where ρ_0, ρ_∞, l are positive parameters, and $\rho_0 > \rho_\infty$. This function introduces the funnel to prescribe the behavior of $\varrho^{\psi}(x,0)$. Our objective is to design $\rho(t), \varrho^{\star}$ such that the satisfaction of (57) implies $\varrho^{\phi}(x,0) > 0$. The selection of these parameters has been explained in detail in [96]. We further define $e(x) = \varrho^{\psi}(x,0) - \varrho^{\star}$, and the modulated error $\bar{e}(x,t) = \frac{e(x)}{\rho(t)}$ with the associated prescribed performance region $\mathcal{D} := \{\bar{e} : \bar{e} \in (-1,0)\}$. Then the modulated error is transformed through a transformation function T, and is defined as

$$\varepsilon(x,t) = T(\bar{e}(x,t)) = \ln\left(-\frac{1+\bar{e}(x,t)}{\bar{e}(x,t)}\right). \tag{58}$$

It can be verified that if the transformed error $\varepsilon(x,t)$ remains bounded, the satisfaction of (57) can be achieved.

We then derive a control strategy for the leader-follower multi-agent system such that the prescribed behavior on $\varrho^{\psi}(x,0)$, as expressed in (57) can be achieved, which will be utilized later for the more complex sequential STL formulas. Prior to presenting the main results, we first state the following assumption that is assumed in this subsection.

Assumption 2. *The leaders have access to $\frac{\partial \varrho^{\psi}(x,0)}{\partial x_L}$, which involves the knowledge of the robustness function $\varrho^{\psi}(x,0)$ and the corresponding agent states it comprises. In addition $\frac{\partial \varrho^{\psi}(x,0)}{\partial x_L}$ is a nonzero vector.*

Next, we propose a control strategy to ensure that $\varrho^{\psi}(x,0)$ always remains within the funnel defined by (57).

Theorem 5.1. *[109] Consider the leader-follower multi-agent system* (55)*, given an STL formula* ϕ *as in* (56b)*, with the corresponding* ψ *satisfying Assumption 2. If the initial condition* $\varrho^{\psi}(x(0),0)$ *is within the funnel* (57)*, then the control strategy*

$$u(x,t) = -\varepsilon(x,t)\frac{\partial \varrho^{\psi}(x,0)}{\partial x_L} \tag{59}$$

guarantees the satisfaction of (57) *for all* $t \geq 0$*, where* $\varepsilon(x,t)$ *is the transformed error defined as in* (58)*.*

Based on Theorem 5.1, we proceed to establish conditions for the funnels. The aim is to ensure that meeting (57) will result in the satisfaction of $0 < \varrho^{\phi}(x,0) < \varrho^{\star}$. This is generally achieved by prescribing the transient behavior of the funnel. We first define the so-called crossing time as

$$t_{\star} = \begin{cases} a & \text{if } \phi = \mathrm{G}_{[a,b]}\psi; \\ a' & \text{if } \phi = \mathrm{F}_{[a,b]}\psi, \end{cases} \tag{60}$$

where $a' \in [a,b]$. The crossing time $t_{\star}$ characterizes the moment when the funnel, defined by the function $-\rho(t) + \varrho^{\star}$, passes through zero. When dealing with the "always" operator $\phi = \mathrm{G}_{[a,b]}\psi$, it is necessary that $\varrho^{\phi}(x(t),0) > 0$ for all $t \in [a,b]$. This requirement leads us to set the crossing time as $t_{\star} = a$. As long as $-\rho(t_{\star}) + \varrho^{\star} = 0$, it follows that $-\rho(t) + \varrho^{\star} > 0, \forall t \in (a,b]$, given that the function $-\rho(t) + \varrho^{\star}$ is strictly increasing. Similarly, when considering the "eventually" operator $\phi = \mathrm{F}_{[a,b]}\psi$, the condition is relaxed to only require the existence of $t \in [a,b]$ such that $\varrho^{\phi}(x,0) > 0$. Therefore, we set the crossing time as $t_{\star} = a' \in [a,b]$ for $\phi = \mathrm{F}_{[a,b]}\psi$. Now, let us recall the performance function $\rho(t) := (\rho_0 - \rho_{\infty})e^{-lt} + \rho_{\infty}$. The following theorem demonstrates how to select the parameters ρ_0, ρ_{∞}, and l to guarantee that satisfying (57) ensures $(x,t) \models \phi$.

Theorem 5.2. *[109] Consider the leader-follower multi-agent system* (55)*, given an STL formula* ϕ *as in* (56b) *with the corresponding* ψ *satisfying Assumption 2. If the initial condition* $\varrho^{\psi}(x(0),0)$ *is within the funnel* (57)*, and it further holds that*

- *for* $t_{\star} = 0$*,* $\rho_0 \in (\varrho^{\star} - \varrho^{\psi}(x(0),0), \varrho^{\star}]$*;* $\rho_{\infty} \in (0, \min(\rho_0, \varrho^{\star}))$*;* $l > 0$*;* $\varrho^{\star} > \varrho^{\psi}(x(0),0)$*.*
- *for* $t_{\star} > 0$*,* $\rho_0 \in (\varrho^{\star} - \varrho^{\psi}(x(0),0), \infty)$*;* $\rho_{\infty} \in (0, \min(\rho_0, \varrho^{\star}))$*;* $l = -\frac{1}{t_{\star}} \ln(\frac{\varrho^{\star} - \rho_{\infty}}{\rho_0 - \rho_{\infty}})$*;* $\varrho^{\star} > \varrho^{\psi}(x(0),0)$*.*

Then, the control strategy (59) *guarantees that* $0 < \varrho^{\phi}(x,0) < \varrho^{\star}$ *holds.*

We then design a hybrid control strategy for the leader-follower multi-agent system (55) to ensure satisfaction of the sequential STL formula presented in (56c). The sequential STL formula $\phi' := \bigwedge_{i=1}^{M} \phi_i$ is composed of M STL formulas of the form (56b). The control strategy for these individual STL formulas has been discussed. The time intervals $[a_i, b_i]$ associated with the basic STL formulas satisfy $b_i \leq a_{i+1}, \forall i \in \{1, \cdots, M-1\}$. For each basic STL formula $\phi_i, i \in \{1, \cdots, M\}$ expressed as $\phi_i = \mathrm{G}_{[a_i,b_i]}\psi_i$ or $\phi_i = \mathrm{F}_{[a_i,b_i]}\psi_i$, we denote its robustness function as $\varrho^{\phi_i}(x,0)$, and the corresponding robustness function $\varrho^{\psi_i}(x,0)$ with respect to ψ_i. The design of the funnel for each $\varrho^{\psi_i}(x,0)$ is carried out as follows:

$$-\rho_i(t) + \varrho_i^{\star} < \varrho^{\psi_i}(x,0) < \varrho_i^{\star}, \tag{61}$$

with $\varrho_i^{\star}$ being a positive scalar and $\rho_i(t) := (\rho_{0,i} - \rho_{\infty,i})e^{-l_i(t-\tau_i)} + \rho_{\infty,i}$, where τ_i are the switching moments that will be defined afterwards. Next, We define $e_i(x) = \varrho^{\psi_i}(x,0) - \varrho_i^{\star}$, the modulated error $\bar{e}_i(x,t) = \frac{e_i(x)}{\rho_i(t)}$, and the transformed error $\varepsilon_i(x,t) = T_i(\bar{e}_i(x,t)) = \ln\left(-\frac{1+\bar{e}_i(x,t)}{\bar{e}_i(x,t)}\right)$. All these parameters are defined in a similar manner. Additionally, for each ϕ_i, we define the crossing time as

$$t_{\star,i} = \begin{cases} a_i & \text{if } \phi_i = \mathrm{G}_{[a_i,b_i]}\psi_i; \\ a_i' & \text{if } \phi_i = \mathrm{F}_{[a_i,b_i]}\psi_i, \end{cases} \tag{62}$$

with $a_i' \in [a_i, b_i]$. At any given moment, only one basic STL formula ϕ_i is active. The transition from ϕ_i to ϕ_{i+1}, where $i \in 1, \cdots, M-1$, occurs once ϕ_i is satisfied. We define the switching moments as $\tau_1, \cdots, \tau_M$, with $\tau_1 = 0$ and $\tau_i \leq \tau_{i+1}$. Here, τ_i represents the moment when the basic STL formula ϕ_i becomes active. For $i \in 2, \cdots, M$, we have that

$$\tau_i = \begin{cases} b_{i-1} & \text{if } \phi_{i-1} = \mathrm{G}_{[a_{i-1},b_{i-1}]}\psi_{i-1}; \\ t_{\star,i-1} & \text{if } \phi_{i-1} = \mathrm{F}_{[a_{i-1},b_{i-1}]}\psi_{i-1}. \end{cases} \tag{63}$$

Drawing upon Theorems 5.1 and 5.2, we present a hybrid control strategy designed to fulfill sequential STL formulas as in (56c).

Theorem 5.3. *[109] Consider the leader-follower multi-agent system* (55)*, given a sequential STL formula* ϕ' *as in* (56c) *such that Assumption 2 holds for each* ψ_i*. Assume that the following conditions hold for all* $i \in \{1, \cdots, M\}$*:*

- *for* $t_{\star,i} - \tau_i = 0$*,* $\rho_{0,i} \in (\varrho_i^{\star} - \varrho^{\psi_i}(x(\tau_i),0), \varrho_i^{\star}]$*;* $\rho_{\infty,i} \in (0, \min(\rho_{0,i}, \varrho_i^{\star}))$*;* $l_i > 0$*;* $\varrho_i^{\star} > \varrho^{\psi_i}(x(\tau_i),0)$*.*
- *for* $t_{\star,i} - \tau_i > 0$*,* $\rho_{0,i} \in (\varrho_i^{\star} - \varrho^{\psi_i}(x(\tau_i),0), \infty)$*;* $\rho_{\infty,i} \in (0, \min(\rho_{0,i}, \varrho_i^{\star}))$*;* $l_i = -\frac{1}{t_{\star,i} - \tau_i} \ln(\frac{\varrho_i^{\star} - \rho_{\infty,i}}{\rho_{0,i} - \rho_{\infty,i}})$*;* $\varrho_i^{\star} > \varrho^{\psi_i}(x(\tau_i),0)$*.*

Let $i \in \{1, \cdots, M-1\}$*, then the hybrid control strategy*

$$u(x,t) = \begin{cases} -\varepsilon_i(x,t)\frac{\partial \varrho^{\psi_i}(x,0)}{\partial x_L}, & t \in [\tau_i, \tau_{i+1}); \\ -\varepsilon_M(x,t)\frac{\partial \varrho^{\psi_M}(x,0)}{\partial x_L}, & t \in [\tau_M, b_M]. \end{cases} \tag{64}$$

guarantees that $0 < \varrho^{\phi_i}(x,0) < \varrho_i^{\star}$ *holds for all* $t \in [\tau_i, \tau_{i+1}], i \in \{1, \cdots, M-1\}$ *and for all* $t \in [\tau_M, b_M]$*, thus* $(x,t) \models \phi'$*.*

5.2. Control of coupled leader-follower subsystems under local STL specifications

In this subsection, we address the challenge of cooperative control in heterogeneous leader-follower multi-agent systems with local STL specifications in a distributed fashion. The entire system is comprised by multiple leader-follower subsystems with coupled dynamics. Only the leaders have knowledge of the relevant STL specifications and are tasked with guiding the followers to ensure global satisfaction of these specifications. Under the assumption of local feasibility, we introduce a funnel-based control methodology for each leader-follower subsystem such that the local STL specifications are achieved, which further implies the global satisfaction of all STL specifications. The discussion in this subsection relies on reference [110].

We consider M leader-follower multi-agent subsystems $\mathcal{S}_i$ under undirected communication graphs $\mathcal{G}_i = (\mathcal{V}_i, \mathcal{E}_i), i \in \mathcal{I} = \{1, \dots, M\}$ with the cardinality of $\mathcal{V}_i$ as $|\mathcal{V}_i| = n_i$ and $\sum_{i\in\mathcal{I}} n_i = N$. Then, the respective vertices sets are indexed as $\mathcal{V}_i = \Big\{(\sum_{j=1}^{i} n_j) - n_i + 1, \dots, \sum_{j=1}^{i} n_j\Big\}$. The edge sets are $\mathcal{E}_i = \{(a,b) \in \mathcal{V}_i \times \mathcal{V}_i \mid b \in \mathcal{N}_a \subset \mathcal{V}_i\}$ where $\mathcal{N}_a \subset \mathcal{V}_i$ denotes the neighbor of agent a in set $\mathcal{V}_i$ such that agent $b \in \mathcal{N}_a$ can communicate with a. Suppose that for each subsystem we have n_i^L leader agents and n_i^F follower agents with the respective vertices set as $\mathcal{V}_i^L = \Big\{(\sum_{j=1}^{i} n_j) - n_i^L + 1, \dots, \sum_{j=1}^{i} n_j\Big\}$ and $\mathcal{V}_i^F = \mathcal{V}_i \setminus \mathcal{V}_i^L$ where it holds that $n_i = n_i^L + n_i^F$. The indexing of agents is performed without loss of generality.

Assuming that the overall leader-follower multi-agent system $\mathcal{S}$ is a composite of the aforementioned leader-follower subsystems under the connected and undirected graph $\mathcal{G} = (\mathcal{V}, \mathcal{E})$ with $\mathcal{V} = \cup_{i\in\mathcal{I}}\mathcal{V}_i$ and $\mathcal{E} = \cup_{i\in\mathcal{I}}\mathcal{E}_i \cup \mathcal{E}_c$. Here, $\mathcal{E}_c = \{(a,b) \in \mathcal{V}_i \times \mathcal{V}_j \mid b \in \mathcal{N}_a \subset \mathcal{V}, i \neq j\}$ represents the edge set connecting distinct subsystems $\mathcal{S}_i, \mathcal{S}_j, i \neq j$. The graph $\mathcal{G}$ is considered connected, implying that there exists a path from any subsystem $\mathcal{S}_i$ to any other subsystem $\mathcal{S}_j$. We can further define the respective leader and follower agents sets of $\mathcal{G}$ as $\mathcal{V}^L = \cup_{i\in\mathcal{I}}\mathcal{V}_i^L$, $\mathcal{V}^F = \cup_{i\in\mathcal{I}}\mathcal{V}_i^F$ and $\mathcal{V} = \mathcal{V}^L \cup \mathcal{V}^F$. Now the neighbor of agent a in set $\mathcal{V}$ is defined as $\mathcal{N}_a = \{b \in \mathcal{V} \mid (a,b) \in \mathcal{E}\}$.

Let $x_k \in \mathbb{R}^n$ be the state of agent $k \in \mathcal{V}$. The state evolution of agent k is governed by the following dynamics:

$$\dot{x}_k = \sum_{l\in\mathcal{N}_k} (x_l - x_k) + b_k u_k, \tag{65}$$

with $b_k = 1$ if $k \in \mathcal{V}^L$, and $b_k = 0$ if $k \in \mathcal{V}^F$. This implies that only the leader controllers will be designed to ensure the global satisfaction of all the STL tasks.

For each leader-follower subsystem $\mathcal{S}_i, i \in \mathcal{I}$, we obtain the dynamics of $\mathcal{S}_i$ by stacking (65) for $k \in \mathcal{V}_i$:

$$\mathcal{S}_i : \dot{\boldsymbol{x}}_{\boldsymbol{i}} = -(L_i \otimes I_n)\boldsymbol{x}_{\boldsymbol{i}} + (C_i \otimes I_n)\boldsymbol{x} + (B_i \otimes I_n)\boldsymbol{u}_{\boldsymbol{i}}, \tag{66}$$

where $\boldsymbol{x}_{\boldsymbol{i}} \in \mathbb{R}^{nn_i}$ is the stacked state of all $x_k, k \in \mathcal{V}_i$, $\boldsymbol{u}_{\boldsymbol{i}} \in \mathbb{R}^{nn_i^L}$ is the input for $\mathcal{S}_i$ by stacking $u_k, k \in \mathcal{V}_i^L$, $\boldsymbol{x} = [\boldsymbol{x}_{\boldsymbol{1}}, \dots, \boldsymbol{x}_{\boldsymbol{M}}]^T \in \mathbb{R}^{nN}$, $L_i \in \mathbb{R}^{n_i \times n_i}$ is the graph Laplacian [97] for $\mathcal{G}_i$, $C_i \in \mathbb{R}^{n_i \times N}$ represents the dynamic couplings between $\mathcal{S}_i$ and $\mathcal{S}_j$ indicated through $\mathcal{E}_c$, $j \in \mathcal{I} \setminus \{i\}$, and $B_i = \begin{bmatrix} 0_{n_i^F \times n_i^L} \\ I_{n_i^L} \end{bmatrix}$. The overall dynamics of the leader-follower multi-agent system $\mathcal{S}$ can be determined similarly as follows:

$$\mathcal{S} : \dot{\boldsymbol{x}} = -(L \otimes I_n)\boldsymbol{x} + (B \otimes I_n)\boldsymbol{u}, \tag{67}$$

with $\boldsymbol{u} = [\boldsymbol{u}_{\boldsymbol{1}}, \dots, \boldsymbol{u}_{\boldsymbol{M}}]^T \in \mathbb{R}^{nn^L}$ and $n^L = \sum_{i=1}^{M} n_i^L$, $L = diag(L_1, \dots, L_M) + [C_1^T, \dots, C_M^T]^T$ is the graph Laplacian of $\mathcal{G}$, and $B = \mathrm{diag}(B_1, \dots, B_M)$.

We then consider the following fragment of the STL specifications:

$$\psi := \top \mid \mu \mid \neg\mu \mid \psi_1 \wedge \psi_2 \tag{68a}$$

$$\phi := \mathrm{F}_{[a,b]}\psi \mid \mathrm{G}_{[a,b]}\psi \mid \mathrm{F}_{[a,b]}\mathrm{G}_{[c,d]}\psi \tag{68b}$$

where ψ in (68b) and ψ_1, ψ_2 in (68a) are non-temporal formulas of class ψ as in (68a), and where ϕ as in (68b) are temporal formulas with $[a,b], [c,d]$ as the time intervals.

Each subsystem $\mathcal{S}_i$ is assigned with one local STL formula $\phi_i, i \in \mathcal{I}$ as in (68b), which can be further decomposed to n_i^L local STL formulas $\phi_i^k, i \in \mathcal{I}, k \in \mathcal{V}_i^L$ as in (68b) corresponding to each leader of $\mathcal{S}_i$ (if $\mathcal{S}_i$ has multiple leaders). The local STL formula ϕ_i^k is only known to the leader $k \in \mathcal{V}_i^L$ in $\mathcal{S}_i$. The local satisfaction of ϕ_i^k depends on only one leader, i.e., k and the neighboring agents of leader k in $\mathcal{S}_i$, which is a subset of agents $\mathcal{V}_{\phi_i^k}$ in $\mathcal{S}_i$, i.e., $\mathcal{V}_{\phi_i^k} \cap \mathcal{V}_i^L = \{k\}$, $\mathcal{V}_{\phi_i^k} \subseteq (\mathcal{N}_k \cap \mathcal{V}_i \cup \{k\}) \subseteq \mathcal{V}_i$. For each leader $k \in \mathcal{V}_i^L$ of the subsystem $\mathcal{S}_i$ which has multiple leaders, we assume that there exists another leader $j \in \mathcal{V}_i^L$ of the same subsystem such that $\mathcal{V}_{\phi_i^k} \cap \mathcal{V}_{\phi_i^j} \neq \emptyset$. This means that for each subsystem $\mathcal{S}_i$, the local STL specifications are coupled within $\mathcal{S}_i$. Otherwise, if $\forall j \in \mathcal{V}_i^L \setminus \{k\}$ for the same subsystem such that $\mathcal{V}_{\phi_i^k} \cap \mathcal{V}_{\phi_i^j} = \emptyset$, we can further decompose the subsystem $\mathcal{S}_i$ into a subsystem with agent set $\mathcal{V}_{\phi_i^k}$ and a subsystem with agent set $\mathcal{V}_i \setminus \mathcal{V}_{\phi_i^k}$. Therefore, the subsystems are defined based on the task dependency, i.e., $\forall k \in \mathcal{V}_i^L, \exists j \in \mathcal{V}_i^L \setminus \{k\}$ such that $\mathcal{V}_{\phi_i^k} \cap \mathcal{V}_{\phi_i^j} \neq \emptyset$. Furthermore, the local satisfaction of ϕ_i depends on a subset of agents $\mathcal{V}_{\phi_i}$ in $\mathcal{S}_i$, i.e., $\mathcal{V}_{\phi_i} \subseteq \mathcal{V}_i$, and also depends on the dynamic couplings with $\mathcal{S}_j, j \in \mathcal{I} \setminus \{i\}$ which are indicated by C_i as in (66). Next, we define the notion of local feasibility as follows.

Definition 9. *(Local satisfaction and local feasibility) The closed-loop signal $\boldsymbol{x}_{\boldsymbol{i}} : [0,\infty) \to \mathbb{R}^{nn_i}$ of $\mathcal{S}_i$ as in (66) locally satisfies ϕ_i if and only if $(\boldsymbol{x}_{\boldsymbol{i}}, 0) \models \phi_i$. The formula ϕ_i for $\mathcal{S}_i$ is locally feasible if and only if $\exists \boldsymbol{u}_{\boldsymbol{i}} : [0,\infty) \to \mathbb{R}^{nn_i^L}$ for (66) such that the closed-loop signal $\boldsymbol{x}_{\boldsymbol{i}} : [0,\infty) \to \mathbb{R}^{nn_i}$ locally satisfies ϕ_i.*

If $\forall i \in \mathcal{I}$, $\boldsymbol{x}_{\boldsymbol{i}}$ locally satisfies ϕ_i for all subsystems $\mathcal{S}_i, i \in \mathcal{I}$, we say that the signal $\boldsymbol{x} : [0,\infty) \to \mathbb{R}^{nN}$ globally satisfies $\{\phi_1, \dots, \phi_M\}$. The set of STL formulas

$\{\phi_1, \ldots, \phi_M\}$ is globally feasible if $\exists \boldsymbol{u} : [0, \infty) \to \mathbb{R}^{nn^L}$ for (67) such that the closed-loop signal $\boldsymbol{x} : [0, \infty) \to \mathbb{R}^{nN}$ globally satisfies $\{\phi_1, \ldots, \phi_M\}$. The objective is to design the local control strategy for each subsystems $\mathcal{S}_i$ as in (66) under the local feasibility assumption as indicated in Assumption 3 such that the closed-loop trajectory $\boldsymbol{x}$ of the leader-follower multi-agent system (67) globally satisfies the STL formulas $\{\phi_1, \ldots, \phi_M\}$.

Assumption 3. *The local STL formula ϕ_i for each subsystem $\mathcal{S}_i, i \in \mathcal{I}$ is locally feasible as per Definition 9.*

Similar to the previous subsection, we can synthesize a control strategy $\boldsymbol{u_i}$ for the subsystem $\mathcal{S}_i, i \in \mathcal{I}$ as in (66) ensuring the fulfillment of local STL formula ϕ_i as in (68b). In cases where $\mathcal{S}_i$ contains more than one leader, we proceed by further decomposing ϕ_i to n_i^L local STL formulas $\phi_i^k, k \in \mathcal{V}_i^L$ for each leader according to the task dependency. Consider the temporal formula ϕ_i as defined in (68b), where the non-temporal formula ψ_i is expressed as $\psi_i = \psi_{i,1} \wedge \cdots \wedge \psi_{i,q}$. Let $\phi_i^k, k \in \mathcal{V}_i^L$ consist only of the formulas $\psi_{i,j}, j \in \{1, \ldots, q\}$ and $\mathcal{V}_{\psi_{i,j}} \subseteq (\mathcal{V}_{\phi_i} \cap \mathcal{N}_k \cup \{k\})$. Here, $\mathcal{V}_{\psi_{i,j}}$ represents the agents involved in $\psi_{i,j}$. If ϕ_i^k contains conjunctions of the non-temporal formulas as in (68a), such as $\phi_i^k := \mathrm{F}_{[a_i,b_i]}\psi_i^k$ and $\psi_i^k := \psi_{i,1}^k \wedge \cdots \wedge \psi_{i,n}^k$, the non-smooth robust semantics $\varrho^{\psi_{i,1}^k \wedge \cdots \wedge \psi_{i,n}^k}(\mathrm{x}, t)$ can be replaced by a smooth under-approximation $\varrho^{\psi_{i,1}^k \wedge \cdots \wedge \psi_{i,n}^k}(\mathrm{x}, t) \approx -\frac{1}{\eta} \ln(\sum_{j=1}^{n} \exp(-\eta \varrho^{\psi_{i,j}^k}(\mathrm{x}, t)))$. Subsequently, we employ prescribed performance control to ensure the fulfillment of temporal STL formulas by prescribing the transient behavior of the non-temporal STL formulas within a predefined region, as described below:

$$-\rho_i^k(t) + \varrho_i^k < \varrho^{\psi_i^k}(\boldsymbol{x_i}, 0) < \varrho_i^k, \quad i \in \mathcal{I}, k \in \mathcal{V}_i^L \tag{69}$$

where ψ_i^k is the corresponding non-temporal formula inside the F, G operators as in (68b). Similarly, we set $\rho_i^k(t) := (\rho_{i,0}^k - \rho_{i,\infty}^k)e^{-l_i^k t} + \rho_{i,\infty}^k$ with funnel parameters $\rho_{i,0}^k, \rho_{i,\infty}^k, l_i^k$ similar to those in (57). We then define the error term $e_i^k(\boldsymbol{x_i}) = \varrho^{\psi_i^k}(\boldsymbol{x_i}, 0) - \varrho_i^k$ and the modulated error as

$$\bar{e}_i^k(\boldsymbol{x_i}, t) = \frac{e_i^k(\boldsymbol{x_i})}{\rho_i^k(t)}. \tag{70}$$

Then, the transformed error is defined via the transformation function T_i^k as

$$\varepsilon_i^k(\boldsymbol{x_i}, t) = T_i^k(\bar{e}_i^k(\boldsymbol{x_i}, t)) := \ln\left(-\frac{1 + \bar{e}_i^k(\boldsymbol{x_i}, t)}{\bar{e}_i^k(\boldsymbol{x_i}, t)}\right). \tag{71}$$

We can apply a similar control strategy based on funnels for each leader-follower subsystem $\mathcal{S}_i, i \in \mathcal{I}$ such that the prescribed behavior on $\varrho^{\psi_i^k}(\boldsymbol{x_i}, 0)$ described as (69) can be achieved. Then, by selecting suitable funnel parameters, we can further guarantee the transient behavior that is characterized by the temporal formulas (68b).

The connection between the non-temporal formulas (68a) and the temporal formulas (68b) is established through the design of the funnel parameters. This design ensures that satisfying (69) guarantees $0 < \varrho^{\phi_i^k}(\boldsymbol{x_i}, 0) < \varrho_i^k$. For each temporal STL formula ϕ_i for $\mathcal{S}_i, i \in \mathcal{I}$ in the form of (68b), the crossing time is defined as

$$t_{\star,i} = \begin{cases} a_i & \text{if } \phi_i = \mathrm{G}_{[a_i,b_i]}\psi_i; \\ a_i' & \text{if } \phi_i = \mathrm{F}_{[a_i,b_i]}\psi_i, \\ a_i'' & \text{if } \phi_i = \mathrm{F}_{[a_i,b_i]}\mathrm{G}_{[c_i,d_i]}\psi_i \end{cases} \tag{72}$$

with $a_i' \in [a_i, b_i]$ and $a_i'' \in [a_i + c_i, b_i + c_i]$. Note that for the subsystem $\mathcal{S}_i$ which has multiple leaders, the decomposed STL formulas $\phi_i^k, k \in \mathcal{V}_i^L$ will share the same time interval.

In this subsection, we make the following assumption, which highlights the advanced capabilities of the leaders.

Assumption 4. *Only the leaders $k \in \mathcal{V}_i^L$ of the leader-follower subsystem $\mathcal{S}_i$ know $\phi_i^k, i \in \mathcal{I}$. In addition $\frac{\partial \varrho^{\psi_i^k}(\boldsymbol{x_i}, 0)}{\partial x_k}, k \in \mathcal{V}_i^L$ is a nonzero vector.*

The following theorem ensures that $\varrho^{\psi_i^k}(\boldsymbol{x_i}, 0)$ remains within the funnel (69) for all $i \in \mathcal{I}, k \in \mathcal{V}_i^L$. Moreover, by appropriately selecting the funnel parameters $\rho_{i,0}^k, \rho_{i,\infty}^k$ and l_i^k, the satisfaction of (69) for all $k \in \mathcal{V}_i^L$ ensures that $(\boldsymbol{x_i}, t) \models \phi_i$.

Theorem 5.4. *[110] Given a local STL formula ϕ_i as in* (68b) *for each leader-follower subsystem $\mathcal{S}_i, i \in \mathcal{I}$ as in* (66) *with the decomposed local STL formula ϕ_i^k for each leader $k \in \mathcal{V}_i^L$. Suppose that Assumptions 3 and 4 hold. If the initial conditions $\varrho^{\psi_i^k}(\boldsymbol{x_i}(0), 0)$ are within the funnel* (69)*, and it further holds that*

- *for $t_{\star,i} = 0$, $\rho_{i,0}^k \in (\varrho_i^k - \varrho^{\psi_i^k}(\boldsymbol{x_i}(0), 0), \varrho_i^k]$; $\rho_{i,\infty}^k \in (0, \min(\rho_{i,0}^k, \varrho_i^k))$; $l_i^k > 0$; $\varrho_i^k > \varrho^{\psi_i^k}(\boldsymbol{x_i}(0), 0)$;*
- *for $t_{\star,i} > 0$, $\rho_{i,0}^k \in (\varrho_i^k - \varrho^{\psi_i^k}(\boldsymbol{x_i}(0), 0), \infty)$; $\rho_{i,\infty}^k \in (0, \min(\rho_{i,0}^k, \varrho_i^k))$; $l_i^k = -\frac{1}{t_{\star,i}} \ln(\frac{\varrho_i^k - \rho_{i,\infty}^k}{\rho_{i,0}^k - \rho_{i,\infty}^k})$; $\varrho_i^k > \varrho^{\psi_i^k}(\boldsymbol{x_i}(0), 0)$,*

then the control strategy

$$u_k(\boldsymbol{x_i}, t) = -\varepsilon_i^k(\boldsymbol{x_i}, t)\frac{\partial \varrho^{\psi_i^k}(\boldsymbol{x_i}, 0)}{\partial x_k}, \quad i \in \mathcal{I}, k \in \mathcal{V}_i^L \tag{73}$$

for each subsystem $\mathcal{S}_i$ guarantees that the closed-loop trajectory $\boldsymbol{x} : [0, \infty) \to \mathbb{R}^{nN}$ of (67) *globally satisfies $\{\phi_1, \ldots, \phi_M\}$, where $\varepsilon_i^k(\boldsymbol{x_i}, t)$ is the transformed error defined as in* (71)*.*

The advancements, in contrast to the previous subsection, involve the integration of coupled dynamics among various subsystems and the inclusion of coupled local STL tasks within each subsystem. Imagine a leader-follower network that is divided into multiple leader-follower subgroups, with specific local tasks assigned to each subgroup.

Coordinating these subtasks is crucial to accomplishing the overall global STL task. This approach is relevant in scenarios where a bottom-up approach is adopted, and different subgroups have already been assigned individual tasks independently, showcasing both a distributed and scalable nature.

5.3. Control of multi-agent systems under STL specifications with an application to cooperative manipulation

In this subsection, we address the problem of cooperative manipulation of an object whose tasks are defined by an STL formula. This subsection is based on the discussions presented in [111]. We make use of the PPC methodology, presented in Subsection 3.2, to enforce transient constraints as required by the STL formula. This is achieved by defining time-varying funnels, ensuring that as long as the states evolve within these funnels, the STL tasks are met. The STL syntax we consider here is

$$\psi ::= \top \mid \mu \mid \neg\mu \tag{74a}$$
$$\phi ::= \psi \mid \mathrm{G}_{[a,b]}\psi \mid \mathrm{F}_{[a,b]}\psi \mid \phi_1 \wedge \phi_2 \mid \phi_1 \vee \phi_2 \tag{74b}$$

where ψ, ψ_1 and ψ_2 are formulae of class ψ given in (74a), ϕ_1, ϕ_2 are formulae of class ϕ given in (74b) and $a, b \in \mathbb{R}_{\geq 0}$ with $a \leq b$. We express the STL syntax (74) in the following way; let $\phi = \phi_1 \vee \phi_2 \vee \cdots \vee \phi_R$, where each ϕ_i is a conjunction $\phi_i = \phi_{i,1} \wedge \phi_{i,2} \wedge \cdots \wedge \phi_{i,M_i}$, and each $\phi_{i,j}$ is of the form

$$\psi \mid \mathrm{G}_{[a,b]}\psi \mid \mathrm{F}_{[a,b]}\psi, \tag{75}$$

for all $j \in \{1, \ldots, M_i\}$, $i \in \{1, \ldots, R\}$ for positive constants M_i and R and where ψ is a formula of the form (74a). Here, R represents the total disjunction components and M_i represents the total conjunction components. We approach the problem in a bottom-up fashion and first consider a formula $\phi_{i,j}$ of the form (75). For each $\phi_{i,j}$, $i \in \{1, \ldots, R\}$, $j \in \{1, \ldots, M_i\}$, we opportunistically activate it only in the time interval $[a_{i,j}, b_{i,j}]$. In this regard, define the smooth switching functions $\beta_{i,j}(t)$ such that

$$\beta_{i,j}(t) = \begin{cases} 0, & t < t^\star_{i,j} - \delta \\ 1, & t \in [t^\star_{i,j}, b_{i,j}] \\ 0, & t > b_{i,j} + \delta, \end{cases} \tag{76}$$

where $\delta > 0$ is the "rise and fall" time, and if there are no temporal constraints we set $\beta_{i,j}(t) = 1$. The smoothness arises from the δ interval, which allows for a smooth transition between 0 and 1. The crossing times $t^\star_{i,j} \in \mathbb{R}_{\geq 0}$ are decided a priori as

$$t^\star_{i,j} \in \begin{cases} [a_{i,j}] & \text{if } \phi_{i,j} = \mathrm{G}_{[a_{i,j},b_{i,j}]}\psi \\ [a_{i,j}, b_{i,j}] & \text{if } \phi_{i,j} = \mathrm{F}_{[a_{i,j},b_{i,j}]}\psi. \end{cases}$$

Next, by $p_{i,j}(\mathbf{x}_o, t)$ denote the predicate functions that correspond to the predicates $\mu_{i,j}$ of the subformulae (75). Next, along (10) we remap $p_{i,j}(\mathbf{x}_o, t)$ to C^1 functions $h_{i,j}(\mathbf{x}_o, t)$ such that

$$\mu_{i,j} = \begin{cases} \top, & -\gamma_{h_{i,j}}(t) < \bar{h}_{i,j}(\mathbf{x}_o, t) < \gamma_{h_{i,j}}(t), \\ \bot, & \text{otherwise} \end{cases}$$

which implies

$$p_{i,j}(\mathbf{x}(t), t) \geq 0 \Leftrightarrow -\gamma_{h_{i,j}}(t) < \bar{h}_{i,j}(\mathbf{x}_o(t), t) < \gamma_{h_{i,j}}(t), \tag{77}$$

where

$$\bar{h}_{i,j}(\mathbf{x}_0, t) = \beta_{i,j}(t) h_{i,j}(\mathbf{x}_0, t). \tag{78}$$

Here, $\gamma_{h_{i,j}}(t)$ are performance functions of the form $\gamma_{h_{i,j}}(t) = (\gamma^0_{h_{i,j}} - \gamma^\infty_{h_{i,j}}) \exp(-l_{i,j}t) + \gamma^\infty_{h_{i,j}}$ (see (2)) that encapsulate state constraints, and $\beta_{i,j}$ in $\bar{h}_{i,j}$ accommodates the temporal constraints for the subformula of the form $\mathrm{G}_{[a_{i,j},b_{i,j}]}\psi_{i,j}, \mathrm{F}_{[a_{i,j},b_{i,j}]}\psi_{i,j}$; by forcing $h_{i,j}(\mathbf{x}_o, t)$ to evolve within the funnels prescribed by $\gamma_{h_{i,j}}(t)$, we intuitively enforce the satisfaction of the STL task. Apart from achieving satisfaction of the predicates, the PPC formulation allows for greater control over the rate of convergence and robustness of $h_{i,j}(\mathbf{x}_o, t)$, since the latter are explicitly shaped by the user-defined performance functions $\gamma_{h_{i,j}}(t)$. These functions also accommodate the temporal constraints imposed by the operators $\mathrm{G}_{[a_{i,j},b_{i,j}]}, \mathrm{F}_{[a_{i,j},b_{i,j}]}$. For example, let $\phi_{i,j} = \mathrm{G}_{[0,5]}\Big(\|\mathbf{x}_o(t)\| < \epsilon\Big)$. Then, $p_{i,j}(\mathbf{x}_o, t) = \epsilon - \|\mathbf{x}_o\|$, $h_{i,j}(\mathbf{x}_o, t) = \|\mathbf{x}_o\|$, and we choose $\gamma_{h_{i,j}}$ such that $\gamma_{h_{i,j}}(0) = \epsilon$, implying $\gamma_{h_{i,j}}(t) < \epsilon$, for all $t > 0$. Note that, subformulae of the form $\mathrm{G}_{[a_{i,j},b_{i,j}]}\psi$ and ψ must be satisfied initially, i.e., at $t = a_{i,j}$ and $t = 0$, respectively. This is formalized in the next assumption:

Assumption 5. *For every $\phi_{i,j} = \psi$, it holds that $p_{i,j}(\mathbf{x}_o(0), 0) \geq 0$, and for every $\phi_{i,j} = \mathrm{G}_{[a_{i,j},b_{i,j}]}\psi$, it holds that $p_{i,j}(\mathbf{x}_o(a_{i,j}), 0) \geq 0$, $j \in \{1, \ldots, M_i\}$, $i \in \{1, \ldots, R\}$.*

In our bottom-up approach, we have outlined methods for encoding $\phi_{i,j}$. Next, we will separately discuss the treatment of conjunctions and disjunctions.

Conjunctions

Consider the formula $\phi_i = \phi_{i,1} \wedge \phi_{i,2} \wedge \cdots \wedge \phi_{i,M_i}$ with each $\phi_{i,j}$ following the form (75) where $i \in \{1, \ldots, R\}$. Let $\bar{h}_{i,j}(\mathbf{x}_o, t)$ be the predicate function corresponding to each $\phi_{i,j}$, constructed as in (78). Define the vector $\bar{h}_i(\mathbf{x}_o, t) = \begin{bmatrix} \bar{h}_{i,1} & \cdots & \bar{h}_{i,M_i} \end{bmatrix}^\top$; where every $\bar{h}_{i,j}, j \in \{1, \ldots, M_i\}$, must satisfy (77) to guarantee satisfaction of ϕ_i.

The following example illustrates the construction of $\bar{h}_i$.

Example 5.5. *Consider the STL formula $\phi_i = \mathrm{G}_{[0,5]}(\|\mathbf{x}_o - A\|_p < 0.1) \wedge \mathrm{F}_{[0,10]}(\|\mathbf{x}_o - B\|_p < 0.1) \wedge \mathrm{G}_{[10,20]}\Big(\phi_o - \pi < \frac{\pi}{12}\Big) \wedge (\|\mathbf{x}_o - C\|_p < 1)\mathrm{U}_{[20,25]}(\|\mathbf{x}_o - C\|_p < 0.05)$ where A, B and C are some desired positions for $\mathbf{x}_o$. The formula ϕ_i can be broken down into four subtasks, namely, 1)*

$\mathrm{G}_{[0,5]}(\|\mathbf{x}_o - A\|_p < 0.1)$ *which requires the object* x_o *between* $0s$ *and* $5s$ *to match configuration* A *within a margin of* 0.1*; 2)* $\mathrm{F}_{[0,10]}(\|\mathbf{x}_o - B\|_p < 0.1)$ *which requires the object* x_o *between* $0s$ *and* $10s$ *to eventually match configuration* B *within a margin of* 0.1*; 3)* $\mathrm{G}_{[10,20]}\left(\phi_o - \pi < \frac{\pi}{12}\right)$ *requires the object to assume a roll angle of* π *between* $10s$ *and* $20s$ *within a margin of* $\pi/6$*; and finally 4)* $(\|\mathbf{x}_o - C\|_p < 1)\mathrm{U}_{[20,25]}(\|\mathbf{x}_o - C\|_p < 0.05)$ *requires the object to assume configuration* C *with an accuracy of* 1 *until the object gets close enough to* C *within the margin* 0.05 *in the interval* $[20, 25]s$*. The function* $\bar{h}_i(\mathbf{x}_o, t) = [\bar{h}_{i,1}(\mathbf{x}_o, t), \bar{h}_{i,2}(\mathbf{x}_o, t), \bar{h}_{i,3}(\mathbf{x}_o, t), \bar{h}_{i,4}(\mathbf{x}_o, t), \bar{h}_{i,5}(\mathbf{x}_o, t)]^\top$*, corresponding to* ϕ_i*, is of the form,*

$$\bar{h}_i(\mathbf{x}_o, t) = \begin{bmatrix} \beta_{i,1}(t)\ h_{i,1}(\mathbf{x}_o) \\ \beta_{i,2}(t)\ h_{i,2}(\mathbf{x}_o) \\ \beta_{i,3}(t)\ h_{i,3}(\mathbf{x}_o) \\ \beta_{i,4}(t)\ h_{i,4}(\mathbf{x}_o) \\ \beta_{i,5}(t)\ h_{i,5}(\mathbf{x}_o) \end{bmatrix} = \begin{bmatrix} \beta_{i,1}(t)\ \|\mathbf{x}_o - A\|_p \\ \beta_{i,2}(t)\ \|\mathbf{x}_o - B\|_p \\ \beta_{i,3}(t)\ (\phi_o - \pi) \\ \beta_{i,4}(t)\ \|\mathbf{x}_o - C\|_p \\ \beta_{i,5}(t)\ \|\mathbf{x}_o - C\|_p \end{bmatrix},$$

where $M_i = 5$ *and* $\beta_{i,j}(t)$ *are switching functions of the form* (76)*,* $j \in \{1, \ldots, 5\}$*.*

Disjunctions

Finally, we are prepared to address disjunctions of the form $\phi = \phi_1 \vee \phi_2 \vee \cdots \vee \phi_R$ where each ϕ_i is a conjunction of subformulas of the form (75), $i \in \{1, \ldots, R\}$. Recall that each ϕ_i corresponds to a predicate function $h_i(\mathbf{x}_o, t) \in \mathbb{R}^{M_i}$;

Fulfilling any ϕ_i ensures the satisfaction of ϕ, therefore, we adopt a cost metric to initially pick a suitable ϕ_i. We introduce the cost function $J_i(h_i(\mathbf{x}_o, t_0))$, which evaluates the robust fulfillment of STL subtask ϕ_i, where t_0 is the initial time step in subformulas $\phi_{i,j}$, $i \in \{1, \ldots, R\}$, $j \in \{1, \ldots, M_i\}$. An example of J_i is $J_i(h(\mathbf{x}o, t_0)) = \frac{1}{M_i} \sum_{j \in \{1,\ldots,M_i\}} \left| \frac{h_{i,j}(\mathbf{x}_o, t_0)}{\gamma_{i,j}(t_0)} \right|$. This formula selects a ϕ_i that, on average, maintains the greatest distance from the funnel limits at t_0. Subsequently, we pick the subtask ϕ_ℓ where $\ell = \arg\min_i J_i(h_i(\mathbf{x}_o(t_0), t_0))$ to be satisfied. This is done by defining the variable

$$k_\ell(t) = \begin{cases} 1 & \text{if} \quad \ell = \arg\min_i J_i(h(\mathbf{x}_o(t_0), t_0)) \\ 0 & \text{otherwise.} \end{cases}$$

and finally selecting the predicate function for ϕ as $\widetilde{h} = [\widetilde{h}_1^\top, \ldots, \widetilde{h}_R^\top]^\top$, with

$$\widetilde{h}(\mathbf{x}_o, t) = \bar{K}(t) \begin{bmatrix} \bar{h}_1(\mathbf{x}_o, t) & \cdots & \bar{h}_R(\mathbf{x}_o, t) \end{bmatrix}^\top$$

where $\bar{K}(t) = \mathrm{blckdiag}\{[k_i I_{M_i}]_{i \in \{1,\ldots,R\}}\}$ is a block diagonal matrix.

An example of such a strategy is shown below.

Example 5.6. *Consider the STL formula,* $\phi = \left[\mathrm{G}_{[0,5]}(\|\mathbf{x}_o - A\|_p < 0.5) \wedge \mathrm{F}_{[5,10]}(\|\mathbf{x}_o - B\|_p < 0.1)\right] \vee \left[\mathrm{F}_{[5,15]}(\|\mathbf{x}_o - C\|_p < 0.05)\right]$ *where* A, B *and* C *are the desired attainable positions for* $\mathbf{x}_o$*. The predicate function corresponding to* ϕ *is*

$$\widetilde{h}(\mathbf{x}_o, t) = \left[\begin{array}{cc:c} k_1(t) & 0 & 0 \\ 0 & k_1(t) & 0 \\ \hdashline 0 & 0 & k_2(t) \end{array}\right] \left[\begin{array}{c} \beta_1(t)\ \|\mathbf{x}_o - A\|_p \\ \beta_2(t)\ \|\mathbf{x}_o - B\|_p \\ \hdashline \beta_3(t)\ \|\mathbf{x}_o - C\|_p \end{array}\right] \tag{79}$$

Along the lines of Subsection 3.2, we present the decentralized control design that guarantees compliance with the funnel presented above and consequently, satisfaction of the STL task. Before proceeding, we impose the following required assumptions.

Assumption 6. *The object's pose does not result in a singular* $J_{o_r}(x_o(t))$*, i.e.* $\theta_o(t) \in \left(-\frac{\pi}{2}, \frac{\pi}{2}\right)$*, for all* $t \geq 0$*.*

Assumption 7. *The function* $\widetilde{h}(\mathbf{x}_o, t)$ *satisfies the following properties:*

- $\widetilde{h}(\mathbf{x}_o, t)$ *is cont. differentiable in* $\mathbb{M} \times \mathbb{R}_{\geq 0}$ *and* $\widetilde{h}$*,* $\frac{\partial \widetilde{h}}{\partial \mathbf{x}_o}$*, and* $\frac{\partial \widetilde{h}}{\partial t}$ *are uniformly bounded in* t *for all* $\mathbf{x}_o \in \mathbb{M}$*.*
- *For every* $c_1 > 0$*, there exists a* $c_2 > 0$ *such that* $\{\mathbf{x}_o \in \mathbb{M} : \|\widetilde{h}(\mathbf{x}_o, t)\| \leq c_1\} \subset \{\mathbf{x}_o \in \mathbb{M} : \|\mathbf{x}_o\| \leq c_2\}$*.*

Assumption 6 is required [100] for the controllability of the object's pose (see (14a)). Assumption 7 provides simple differentiability and boundedness conditions for $\widetilde{h}$ and that boundedness of $\widetilde{h}(\mathbf{x}_o, t)$ implies the boundedness of $\mathbf{x}_o$.

Next, let ℓ be the index of the chosen subformulae to be satisfied in the disjunction operator, i.e., $k_\ell = 1$ and $k_i = 0$, for all $i \in \{1, \ldots, R\} \backslash \{\ell\}$. Then, the sub task to be satisfied is given by the function $\widetilde{h}_\ell(\mathbf{x_o}, t) = \bar{h}_\ell(\mathbf{x_o}, t) = [\bar{h}_{\ell,1}, \ldots, \bar{h}_{\ell,M_\ell}]^\top$. We provide now the control design.

Step I-a.

Choose the performance functions $\gamma_h(t) = \mathrm{diag}\{\gamma_{h_{\ell,1}}, \gamma_{h_{\ell,2}}, \ldots, \gamma_{h_{\ell,M_\ell}}\}$ and $\gamma_{h_{\ell,j}}(t) = (\gamma^0_{h_{\ell,j}} - \gamma^\infty_{h_{\ell,j}}) \exp(-l_{\ell,j} t) + \gamma^\infty_{h_{\ell,j}}$, with $\gamma^0_{h_{\ell,j}} > \bar{h}_{\ell,j}(\mathbf{x}_o(0), 0)$; $l_{\ell,j} \in \mathbb{R}_{>0}$ and $\gamma^\infty_{h_{\ell,j}}$ are chosen such that, when $-\gamma_{h_{\ell,j}}(t) < \bar{h}_{\ell,j}(\mathbf{x}_o, t) < \gamma_{h_{\ell,j}}(t)$ holds, the task is satisfied, for $j \in \{1, 2, \ldots, M_\ell\}$. In the special case that $\phi_{\ell,j}$ has the form $\|\mathbf{x}_o - A\| < z$, for some $\mathbf{x}_o \in \mathbb{M}$, $z > 0$, we set $\gamma^\infty_{h_{\ell,j}} = z$.

Step I-b. Define the normalised errors $\xi_h \in \mathbb{R}^L$ by

$$\xi_h = [\xi_{h_{\ell,1}}, \ldots, \xi_{h_{\ell,M_\ell}}]^\top = \gamma_h^{-1}(t) \bar{h}_\ell(\mathbf{x}_o, t) \tag{80}$$

and design the reference velocity v_r as

$$v_r(\xi_h, t) = -g_s J_{o_r}(\mathbf{x}_o) \frac{\partial \bar{h}_\ell}{\partial \mathbf{x}_o}^\top \gamma_h^{-1}(t) r_h(\xi_h) \varepsilon_h(\xi_h) \tag{81}$$

where g_s is a positive constant and the signals $\varepsilon_h : (-1, 1)^{M_\ell} \to \mathbb{R}^{M_\ell}$ and $r_h : (-1, 1)^{M_\ell} \to \mathbb{R}^{M_\ell \times M_\ell}$

are $\varepsilon_h(\xi_h) = [\varepsilon_{h_{\ell,1}}(\xi_{h_{\ell,1}}), \ldots, \varepsilon_{h_{\ell,M_\ell}}(\xi_{h_{\ell,M_\ell}})]^\top$, $r_h(\xi_h) = \text{diag}\{[r_{h_{\ell,j}}(\xi_{h_{\ell,j}})]_{j\in\{1,\ldots,M_\ell\}}\}$, with

$$\varepsilon_{h_{\ell,j}} = \ln\Big(\frac{1+\xi_{h_{\ell,j}}}{1-\xi_{h_{\ell,j}}}\Big),\ r_{h_{\ell,j}} = \frac{2}{1-\xi^2_{h_{\ell,j}}},\ j \in \{1,\ldots,M_\ell\}.$$

Step II-a. Define the velocity error $e_v \in \mathbb{R}^6$ as,

$$e_v = [e_{v_1}, \ldots, e_{v_6}]^\top = v_o - v_r(\xi_h, t), \tag{82}$$

and velocity performance functions $\gamma_v(t) = \text{diag}\{\gamma_{v_1}, \gamma_{v_2}, \ldots, \gamma_{v_6}\}$ where $\gamma_{v_n}(t) = (\gamma^0_{v_n} - \gamma^\infty_{v_i})\exp(-l_{v_n}t) + \gamma^\infty_{v_n}$, with parameters $\gamma^0_{v_n} > |e_{v_n}(t_0)|$, $\gamma^\infty_{v_i} \in (0, \gamma^0_{v_n})$ and $l_{v_n} > 0$, $\forall n \in \{1,\ldots,6\}$.

Step II-b. Define the normalised velocity errors $\xi_v \in \mathbb{R}^6$:

$$\xi_v = [\xi_{v_1}, \ldots, \xi_{v_6}]^\top = \gamma_v^{-1}(t)e_v, \tag{83}$$

where $\gamma_v = \text{diag}\{[\gamma_{v_m}]_{m\in\{1,\ldots,6\}}\}$, and design the decentralized control law as

$$u(\xi_h, \xi_v, t) = \begin{bmatrix} u_1(\xi_h, \xi_v, t) \\ \vdots \\ u_N(\xi_h, \xi_v, t) \end{bmatrix} = -C_g G^\star(q)\gamma_v^{-1}(t) r_v(\xi_v)\varepsilon_v(\xi_v) \tag{84}$$

where $G^\star(q) = [J^{-1}_{o_1}(q_1), \ldots, J^{-1}_{o_N}(q_N)] \in \mathbb{R}^{6N\times 6}$, $C_g = g_v\text{diag}\{[c_i I_6]_{i\in\mathcal{N}}\} \in \mathbb{R}^{6N\times 6N}$ and the signals $\varepsilon_v : (-1,1)^6 \to \mathbb{R}^6$ and $r_v : (-1,1)^6 \to \mathbb{R}^{6\times 6}$ are $\varepsilon_v(\xi_v) = [\varepsilon_{v_1}(\xi_{v_1}), \ldots, \varepsilon_{v_6}(\xi_{v_6})]^\top$, $r_v(\xi_v) = \text{diag}\{[r_{v_n}(\xi_{v_n})]_{n\in\{1,\ldots,6\}}\}$, with

$$\varepsilon_{v_n} = \ln\Big(\frac{1+\xi_{v_n}}{1-\xi_{v_n}}\Big),\ r_{v_n} = \frac{2}{1-\xi^2_{v_n}},\ n \in \{1,\ldots,6\}.$$

The control protocol guarantees the normalized errors $\xi_{h_{\ell,j}}$, ξ_{v_i} to remain strictly within $(-1,1)$, which is equivalent to guaranteeing the boundedness of the transformed signals $\varepsilon_{h_{\ell,j}}$, ε_{v_i}, respectively. The correctness of the proposed control scheme is stated in the following theorem.

Theorem 5.7. *[111] Consider N agents rigidly grasping an object with coupled dynamics* (15) *subject to an STL formula ϕ of the form* (74)*. Assume that $\lambda_{\min}\Big(\frac{\partial \bar{h}_\ell}{\partial \mathbf{x}_o}\frac{\partial \bar{h}_\ell}{\partial \mathbf{x}_o}^\top\Big) \geq \kappa > 0$, for all $t \geq 0$. Then the decentralized control* (84) *guarantees $|\bar{h}_{\ell,j}(\mathbf{x}_o(t), t)| < \gamma_{\ell,j}(t)$, for all $t \geq 0$, and the boundedness of all closed loop signals.*

6. Conclusion and discussion

6.1. Conclusion

This paper presented cooperative control and task planning for heterogeneous multi-agent systems under both spatial and temporal constraints. It specifically focuses on a category of heterogeneous leader-follower multi-agent systems as well. Addressing the challenge of distributed control and task planning for such systems within spatiotemporal constraints is unsatisfactorily resolved thus far. This is primarily due to the limitations of current control synthesis approaches based on formal methods, which tend to be either centralized or homogeneous. These approaches are inadequate for accommodating the heterogeneous leader-follower multi-agent systems required in our framework, where different agent capabilities are taken into account. Moreover, the conventional handling of spatiotemporal constraints using standard discrete logics, such as Linear Temporal Logic (LTL), relies on discrete approximations. This approach may be computationally intractable and may not effectively address the spatiotemporal constraints inherent in the continuous dynamics and couplings present in multi-agent systems.

In this article, we present an overview of our efforts to propose a systematic approach to transient control for cooperative objectives in heterogeneous leader-follower networks, demonstrating both a distributed and scalable nature. Afterward, these transient controllers are employed without relying on model checking procedures to handle spatiotemporal logic specifications in a heterogeneous leader-follower setup, highlighting their continuous nature in both time and space.

6.2. Future directions

The investigation into distributed control of heterogeneous leader-follower multi-agent systems under spatiotemporal constraints continues to pose numerous open and highly challenging problems. This encompasses the exploration of alternative transient approaches like control barrier functions and model predictive control. Additionally, efforts are directed towards enhancing the expressivity of STL specifications, investigating the topological conditions of heterogeneous leader-follower networks to ensure the feasibility of spatiotemporal constraints, addressing leader selection problems in the presence of transient constraints, delving into the robustness of the leader-follower networks in terms of agent failures, and exploring network reconfigurations to effectively handle infeasibility and failures.

Declaration of competing interest

The authors declare that they have no known competing financial interests or personal relationships that could have appeared to influence the work reported in this paper.

References

[1] J. A. Fax, R. M. Murray, Information flow and cooperative control of vehicle formations (2003).

[2] M. Gatti, P. Cavalin, S. B. Neto, C. Pinhanez, C. dos Santos, D. Gribel, A. P. Appel, Large-scale multi-agent-based modeling and simulation of microblogging-based online social network, in: International Workshop on Multi-Agent Systems and Agent-Based Simulation, Springer, 2013, pp. 17–33.

[3] V. Gorodetski, I. Kotenko, The multi-agent systems for computer network security assurance: frameworks and case studies, in: Proceedings 2002 IEEE International Conference on Artificial Intelligence Systems (ICAIS 2002), IEEE, 2002, pp. 297–302.

[4] B. Burmeister, A. Haddadi, G. Matylis, Application of multi-agent systems in traffic and transportation, IEE Proceedings-Software 144 (1) (1997) 51–60.

[5] R. Olfati-Saber, J. A. Fax, R. M. Murray, Consensus and cooperation in networked multi-agent systems, Proceedings of the IEEE 95 (1) (2007) 215–233.

[6] T. Balch, R. C. Arkin, Behavior-based formation control for multirobot teams, IEEE transactions on robotics and automation 14 (6) (1998) 926–939.

[7] R. Olfati-Saber, Flocking for multi-agent dynamic systems: Algorithms and theory, IEEE Transactions on automatic control 51 (3) (2006) 401–420.

[8] J. Cortes, S. Martinez, T. Karatas, F. Bullo, Coverage control for mobile sensing networks, IEEE Transactions on robotics and Automation 20 (2) (2004) 243–255.

[9] L. Macellari, Y. Karayiannidis, D. V. Dimarogonas, Multi-agent second order average consensus with prescribed transient behavior, IEEE Transactions on Automatic Control 62 (10) (2017) 5282–5288.

[10] S.-L. Dai, S. He, H. Lin, C. Wang, Platoon formation control with prescribed performance guarantees for usvs, IEEE Transactions on Industrial Electronics 65 (5) (2017) 4237–4246.

[11] C. Baier, J.-P. Katoen, Principles of model checking, MIT press, 2008.

[12] C. Belta, B. Yordanov, E. A. Gol, Formal Methods for Discrete-Time Dynamical Systems, Vol. 89, Springer, 2017.

[13] H. Kress-Gazit, G. E. Fainekos, G. J. Pappas, Temporal-logic-based reactive mission and motion planning, IEEE transactions on robotics 25 (6) (2009) 1370–1381.

[14] O. Maler, D. Nickovic, Monitoring temporal properties of continuous signals, in: Formal Techniques, Modelling and Analysis of Timed and Fault-Tolerant Systems, Springer, 2004, pp. 152–166.

[15] C. P. Bechlioulis, G. A. Rovithakis, Robust adaptive control of feedback linearizable mimo nonlinear systems with prescribed performance, IEEE Transactions on Automatic Control 53 (9) (2008) 2090–2099.

[16] Z. Li, Z. Duan, L. Huang, Leader-follower consensus of multi-agent systems, in: 2009 American control conference, IEEE, 2009, pp. 3256–3261.

[17] W. Cao, J. Zhang, W. Ren, Leader–follower consensus of linear multi-agent systems with unknown external disturbances, Systems & Control Letters 82 (2015) 64–70.

[18] J. Hu, G. Feng, Distributed tracking control of leader–follower multi-agent systems under noisy measurement, Automatica 46 (8) (2010) 1382–1387.

[19] Y. Hong, X. Wang, Z.-P. Jiang, Distributed output regulation of leader–follower multi-agent systems, International Journal of Robust and Nonlinear Control 23 (1) (2013) 48–66.

[20] G. Notarstefano, M. Egerstedt, M. Haque, Containment in leader–follower networks with switching communication topologies, Automatica 47 (5) (2011) 1035–1040.

[21] M. Ji, A. Muhammad, M. Egerstedt, Leader-based multi-agent coordination: Controllability and optimal control, in: American Control Conference, 2006, IEEE, 2006, pp. 6–pp.

[22] M. Pirani, E. M. Shahrivar, B. Fidan, S. Sundaram, Robustness of leader–follower networked dynamical systems, IEEE Transactions on Control of Network Systems 5 (4) (2017) 1752–1763.

[23] H. G. Tanner, On the controllability of nearest neighbor interconnections, in: 43rd IEEE Conference on Decision and Control (CDC), 2004, Vol. 3, IEEE, 2004, pp. 2467–2472.

[24] M. Egerstedt, S. Martini, M. Cao, K. Camlibel, A. Bicchi, Interacting with networks: How does structure relate to controllability in single-leader, consensus networks?, IEEE Control Systems 32 (4) (2012) 66–73.

[25] A. Rahmani, M. Ji, M. Mesbahi, M. Egerstedt, Controllability of multi-agent systems from a graph-theoretic perspective, SIAM Journal on Control and Optimization 48 (1) (2009) 162–186.

[26] D. Goldin, J. Raisch, Controllability of second order leader-follower systems, in: 2nd IFAC Workshop on Distributed Estimation and Control in Networked Systems 2010-NecSys 10, 2010, pp. 233–238.

[27] C. Sun, G. Hu, L. Xie, Controllability of multiagent networks with antagonistic interactions, IEEE Transactions on Automatic Control 62 (10) (2017) 5457–5462.

[28] A. Yazıcıoğlu, W. Abbas, M. Egerstedt, Graph distances and controllability of networks, IEEE Transactions on Automatic Control 61 (12) (2016) 4125–4130.

[29] S. Zhang, M. K. Camlibel, M. Cao, Controllability of diffusively-coupled multi-agent systems with general and distance regular coupling topologies, in: Decision and Control and European Control Conference (CDC-ECC), 2011 50th IEEE Conference on, IEEE, 2011, pp. 759–764.

[30] S. Zhang, M. Cao, M. K. Camlibel, Upper and lower bounds for controllable subspaces of networks of diffusively coupled agents, IEEE Transactions on Automatic control 59 (3) (2014) 745–750.

[31] C. O. Aguilar, B. Gharesifard, Graph controllability classes for the laplacian leader-follower dynamics, IEEE transactions on automatic control 60 (6) (2014) 1611–1623.

[32] A. Y. Yazicioğlu, M. Egerstedt, Leader selection and network assembly for controllability of leader-follower networks, in: American Control Conference (ACC), 2013, IEEE, 2013, pp. 3802–3807.

[33] K. Fitch, N. E. Leonard, Optimal leader selection for controllability and robustness in multi-agent networks, in: 2016 European Control Conference (ECC), IEEE, 2016, pp. 1550–1555.

[34] S. Patterson, B. Bamieh, Leader selection for optimal network coherence, in: 49th IEEE Conference on Decision and Control (CDC), IEEE, 2010, pp. 2692–2697.

[35] S. Patterson, N. McGlohon, K. Dyagilev, Optimal k-leader selection for coherence and convergence rate in one-dimensional networks, IEEE Transactions on Control of Network Systems 4 (3) (2016) 523–532.

[36] M. Fardad, F. Lin, M. R. Jovanović, Algorithms for leader selection in large dynamical networks: Noise-free leaders, in: 2011 50th IEEE Conference on Decision and Control and European Control Conference, IEEE, 2011, pp. 7188–7193.

[37] H. Kawashima, M. Egerstedt, Leader selection via the manipulability of leader-follower networks, in: 2012 American Control Conference (ACC), IEEE, 2012, pp. 6053–6058.

[38] Y. Karayiannidis, D. V. Dimarogonas, D. Kragic, Multi-agent average consensus control with prescribed performance guarantees, in: Decision and Control (CDC), 2012 IEEE 51st Annual Conference on, IEEE, 2012, pp. 2219–2225.

[39] C. P. Bechlioulis, K. J. Kyriakopoulos, Robust model-free formation control with prescribed performance and connectivity maintenance for nonlinear multi-agent systems, in: 53rd IEEE Conference on Decision and Control, IEEE, 2014, pp. 4509–4514.

[40] C. K. Verginis, C. P. Bechlioulis, D. V. Dimarogonas, K. J. Kyriakopoulos, Robust distributed control protocols for large vehicular platoons with prescribed transient and steady-state performance, IEEE Transactions on Control Systems Technology 26 (1) (2018) 299–304.

[41] C. K. Verginis, D. V. Dimarogonas, Adaptive leader-follower coordination of lagrangian multi-agent systems under transient constraints, in: 2019 IEEE 58th Conference on Decision and Control (CDC), IEEE, 2019, pp. 3833–3838.

[42] Y. Karayiannidis, Z. Doulgeri, Model-free robot joint position regulation and tracking with prescribed performance guarantees, Robotics and Autonomous Systems 60 (2) (2012) 214–226.

[43] I. Katsoukis, G. A. Rovithakis, Output feedback leader-follower with prescribed performance guarantees for a

class of unknown nonlinear multi-agent systems, in: 2016 24th Mediterranean Conference on Control and Automation (MED), IEEE, 2016, pp. 1077–1082.
[44] M. Zambelli, Y. Karayiannidis, D. V. Dimarogonas, Posture regulation for unicycle-like robots with prescribed performance guarantees, IET Control Theory & Applications 9 (2) (2015) 192–202.
[45] C. P. Bechlioulis, G. A. Rovithakis, Prescribed performance adaptive control for multi-input multi-output affine in the control nonlinear systems, IEEE Transactions on automatic control 55 (5) (2010) 1220–1226.
[46] C. K. Verginis, A. Nikou, D. V. Dimarogonas, Robust formation control in se (3) for tree-graph structures with prescribed transient and steady state performance, Automatica 103 (2019) 538–548.
[47] L. Lindemann, C. K. Verginis, D. V. Dimarogonas, Prescribed performance control for signal temporal logic specifications, in: 2017 IEEE 56th Annual Conference on Decision and Control (CDC), IEEE, 2017, pp. 2997–3002.
[48] C. K. Verginis, D. V. Dimarogonas, Timed abstractions for distributed cooperative manipulation, Autonomous Robots 42 (4) (2018) 781–799.
[49] M. Guo, C. P. Bechlioulis, K. J. Kyriakopoulos, D. V. Dimarogonas, Hybrid control of multiagent systems with contingent temporal tasks and prescribed formation constraints, IEEE Transactions on Control of Network Systems 4 (4) (2016) 781–792.
[50] A. Ilchmann, E. P. Ryan, C. J. Sangwin, Tracking with prescribed transient behaviour, ESAIM: Control, Optimisation and Calculus of Variations 7 (2002) 471–493.
[51] A. Ilchmann, E. P. Ryan, S. Trenn, Adaptive tracking within prescribed funnels, in: Proceedings of the 2004 IEEE International Conference on Control Applications, 2004., Vol. 2, IEEE, 2004, pp. 1032–1036.
[52] A. Ilchmann, E. P. Ryan, S. Trenn, Tracking control: Performance funnels and prescribed transient behaviour, Systems & Control Letters 54 (7) (2005) 655–670.
[53] T. Berger, H. H. Lê, T. Reis, Funnel control for nonlinear systems with known strict relative degree, Automatica 87 (2018) 345–357.
[54] J. Hu, S. Trenn, X. Zhu, Funnel control for relative degree one nonlinear systems with input saturation, in: 2022 European Control Conference (ECC), IEEE, 2022, pp. 227–232.
[55] C. M. Hackl, N. Hopfe, A. Ilchmann, M. Mueller, S. Trenn, Funnel control for systems with relative degree two, SIAM Journal on Control and Optimization 51 (2) (2013) 965–995.
[56] N. Hopfe, A. Ilchmann, E. P. Ryan, Funnel control with saturation: Linear mimo systems, IEEE Transactions on Automatic Control 55 (2) (2010) 532–538.
[57] N. Hopfe, A. Ilchmann, E. P. Ryan, Funnel control with saturation: Nonlinear siso systems, IEEE Transactions on Automatic Control 55 (9) (2010) 2177–2182.
[58] A. Ilchmann, S. Trenn, Input constrained funnel control with applications to chemical reactor models, Systems & control letters 53 (5) (2004) 361–375.
[59] D. Liberzon, S. Trenn, The bang-bang funnel controller for uncertain nonlinear systems with arbitrary relative degree, IEEE Transactions on Automatic Control 58 (12) (2013) 3126–3141.
[60] H. Shim, S. Trenn, A preliminary result on synchronization of heterogeneous agents via funnel control, in: 2015 54th IEEE Conference on Decision and Control (CDC), IEEE, 2015, pp. 2229–2234.
[61] J. G. Lee, T. Berger, S. Trenn, H. Shim, Edge-wise funnel output synchronization of heterogeneous agents with relative degree one, arXiv preprint arXiv:2110.05330 (2021).
[62] J. G. Lee, S. Trenn, H. Shim, Synchronization with prescribed transient behavior: Heterogeneous multi-agent systems under funnel coupling, Automatica 141 (2022) 110276.
[63] T. Berger, D. Dennstädt, A. Ilchmann, K. Worthmann, Funnel model predictive control for nonlinear systems with relative degree one, SIAM Journal on Control and Optimization 60 (6) (2022) 3358–3383.
[64] T. Berger, D. Dennstädt, Funnel mpc with feasibility constraints for nonlinear systems with arbitrary relative degree, IEEE Control Systems Letters 6 (2022) 2804–2809.
[65] T. Berger, T. Reis, Zero dynamics and funnel control for linear electrical circuits, Journal of the Franklin Institute 351 (11) (2014) 5099–5132.
[66] T. Berger, A.-L. Rauert, Funnel cruise control, Automatica 119 (2020) 109061.
[67] C. Baier, J.-P. Katoen, Principles of Model Checking, MIT press, 2008.
[68] O. Maler, D. Nickovic, Monitoring temporal properties of continuous signals, in: Formal Techniques, Modelling and Analysis of Timed and Fault-Tolerant Systems, Springer, 2004, pp. 152–166.
[69] C. Madsen, P. Vaidyanathan, S. Sadraddini, C.-I. Vasile, N. A. DeLateur, R. Weiss, D. Densmore, C. Belta, Metrics for signal temporal logic formulae, in: 2018 IEEE Conference on Decision and Control (CDC), IEEE, 2018, pp. 1542–1547.
[70] N. Mehdipour, C.-I. Vasile, C. Belta, Specifying user preferences using weighted signal temporal logic, IEEE Control Systems Letters 5 (6) (2020) 2006–2011.
[71] N. Mehdipour, C.-I. Vasile, C. Belta, Average-based robustness for continuous-time signal temporal logic, in: 2019 IEEE 58th Conference on Decision and Control (CDC), IEEE, 2019, pp. 5312–5317.
[72] N. Mehdipour, C.-I. Vasile, C. Belta, Arithmetic-geometric mean robustness for control from signal temporal logic specifications, in: 2019 American Control Conference (ACC), IEEE, 2019, pp. 1690–1695.
[73] Y. Gilpin, V. Kurtz, H. Lin, A smooth robustness measure of signal temporal logic for symbolic control, IEEE Control Systems Letters 5 (1) (2020) 241–246.
[74] I. Haghighi, N. Mehdipour, E. Bartocci, C. Belta, Control from signal temporal logic specifications with smooth cumulative quantitative semantics, in: 2019 IEEE 58th Conference on Decision and Control (CDC), IEEE, 2019, pp. 4361–4366.
[75] G. Yang, C. Belta, R. Tron, Continuous-time signal temporal logic planning with control barrier functions, in: 2020 American Control Conference (ACC), 2020, pp. 4612–4618.
[76] L. Lindemann, D. V. Dimarogonas, Control barrier functions for signal temporal logic tasks, IEEE control systems letters 3 (1) (2018) 96–101.
[77] L. Lindemann, D. V. Dimarogonas, Control barrier functions for multi-agent systems under conflicting local signal temporal logic tasks, IEEE Control Systems Letters 3 (3) (2019) 757–762.
[78] M. Charitidou, D. V. Dimarogonas, Receding horizon control with online barrier function design under signal temporal logic specifications, IEEE Transactions on Automatic Control (2022).
[79] A. T. Buyukkocak, D. Aksaray, Y. Yazıcıoğlu, Control barrier functions with actuation constraints under signal temporal logic specifications, in: 2022 European Control Conference (ECC), IEEE, 2022, pp. 162–168.
[80] W. Xiao, C. A. Belta, C. G. Cassandras, High order control lyapunov-barrier functions for temporal logic specifications, in: 2021 American Control Conference (ACC), IEEE, 2021, pp. 4886–4891.
[81] V. Raman, A. Donzé, D. Sadigh, R. M. Murray, S. A. Seshia, Reactive synthesis from signal temporal logic specifications, in: Proceedings of the 18th international conference on hybrid systems: Computation and control, 2015, pp. 239–248.
[82] V. Raman, A. Donzé, M. Maasoumy, R. M. Murray, A. Sangiovanni-Vincentelli, S. A. Seshia, Model predictive control with signal temporal logic specifications, in: 53rd IEEE Conference on Decision and Control, 2014, pp. 81–87.
[83] S. Sadraddini, C. Belta, Robust temporal logic model predictive control, in: 2015 53rd Annual Allerton Conference on Communication, Control, and Computing (Allerton), IEEE, 2015, pp. 772–779.

[84] C.-I. Vasile, V. Raman, S. Karaman, Sampling-based synthesis of maximally-satisfying controllers for temporal logic specifications, in: 2017 IEEE/RSJ International Conference on Intelligent Robots and Systems (IROS), 2017, pp. 3840–3847.

[85] D. Aksaray, A. Jones, Z. Kong, M. Schwager, C. Belta, Q-learning for robust satisfaction of signal temporal logic specifications, in: 2016 IEEE 55th Conference on Decision and Control (CDC), 2016, pp. 6565–6570.

[86] V. Kurtz, H. Lin, Bayesian optimization for polynomial time probabilistically complete STL trajectory synthesis, arXiv preprint arXiv:1905.03051 (2019).

[87] W. Liu, N. Mehdipour, C. Belta, Recurrent neural network controllers for signal temporal logic specifications subject to safety constraints, IEEE Control Systems Letters 6 (2021) 91–96.

[88] G. Bombara, C. Belta, Offline and online learning of signal temporal logic formulae using decision trees, ACM Transactions on Cyber-Physical Systems 5 (3) (2021) 1–23.

[89] A. Linard, J. Tumova, Active learning of signal temporal logic specifications, in: 2020 IEEE 16th International Conference on Automation Science and Engineering (CASE), IEEE, 2020, pp. 779–785.

[90] H. Venkataraman, D. Aksaray, P. Seiler, Tractable reinforcement learning of signal temporal logic objectives, in: Learning for Dynamics and Control, PMLR, 2020, pp. 308–317.

[91] Z. Lin, J. S. Baras, Optimization-based motion planning and runtime monitoring for robotic agent with space and time tolerances, IFAC-PapersOnLine 53 (2) (2020) 1874–1879.

[92] K. Leung, N. Aréchiga, M. Pavone, Backpropagation through signal temporal logic specifications: Infusing logical structure into gradient-based methods, The International Journal of Robotics Research (2020) 02783649221082115.

[93] A. T. Buyukkocak, D. Aksaray, Y. Yazıcıoğlu, Control synthesis using signal temporal logic specifications with integral and derivative predicates, in: 2021 American Control Conference (ACC), IEEE, 2021, pp. 4873–4878.

[94] A. T. Buyukkocak, D. Aksaray, Y. Yazıcıoğlu, Planning of heterogeneous multi-agent systems under signal temporal logic specifications with integral predicates, IEEE Robotics and Automation Letters 6 (2) (2021) 1375–1382.

[95] L. Lindemann, D. V. Dimarogonas, Funnel control for fully actuated systems under a fragment of signal temporal logic specifications, Nonlinear Analysis: Hybrid Systems 39 (2021) 100973.

[96] L. Lindemann, D. V. Dimarogonas, Feedback control strategies for multi-agent systems under a fragment of signal temporal logic tasks, Automatica 106 (2019) 284–293.

[97] M. Mesbahi, M. Egerstedt, Graph Theoretic Methods in Multiagent Networks, Vol. 33, Princeton University Press, 2010.

[98] G. E. Fainekos, G. J. Pappas, Robustness of temporal logic specifications for continuous-time signals, Theoretical Computer Science 410 (42) (2009) 4262–4291.

[99] A. Donzé, O. Maler, Robust satisfaction of temporal logic over real-valued signals, in: International Conference on Formal Modeling and Analysis of Timed Systems, Springer, 2010, pp. 92–106.

[100] B. Siciliano, O. Khatib, T. Kröger, Springer handbook of robotics, Vol. 200, Springer, 2008.

[101] F. Chen, D. V. Dimarogonas, Consensus control for leader-follower multi-agent systems under prescribed performance guarantees, in: 2019 IEEE 58th Conference on Decision and Control (CDC), IEEE, 2019, pp. 4785–4790.

[102] F. Chen, D. V. Dimarogonas, Leader–follower formation control with prescribed performance guarantees, IEEE Transactions on Control of Network Systems 8 (1) (2020) 450–461.

[103] D. V. Dimarogonas, K. H. Johansson, Stability analysis for multi-agent systems using the incidence matrix: quantized communication and formation control, Automatica 46 (4) (2010) 695–700.

[104] F. Chen, D. V. Dimarogonas, Second order consensus for leader-follower multi-agent systems with prescribed performance, IFAC-PapersOnLine 52 (20) (2019) 103–108.

[105] C. P. Bechlioulis, G. A. Rovithakis, A low-complexity global approximation-free control scheme with prescribed performance for unknown pure feedback systems, Automatica 50 (4) (2014) 1217–1226.

[106] F. Chen, D. V. Dimarogonas, Further results on leader-follower multi-agent formation control with prescribed performance guarantees, in: 2020 59th IEEE Conference on Decision and Control (CDC), IEEE, 2020, pp. 4023–4030.

[107] D. Zelazo, M. Mesbahi, Edge agreement: Graph-theoretic performance bounds and passivity analysis, IEEE Transactions on Automatic Control 56 (3) (2011) 544–555.

[108] F. Chen, D. V. Dimarogonas, On topological conditions for enabling transient control in leader-follower networks, arXiv preprint arXiv:2312.03246 (2023).

[109] F. Chen, D. V. Dimarogonas, Funnel-based cooperative control of leader-follower multi-agent systems under signal temporal logic specifications, in: 2022 European Control Conference (ECC), IEEE, 2022, pp. 906–911.

[110] F. Chen, D. V. Dimarogonas, Distributed control of coupled leader-follower multi-agent systems under spatiotemporal logic tasks, in: IFAC World Congress 2023, 2023.

[111] M. Sewlia, C. K. Verginis, D. V. Dimarogonas, Cooperative object manipulation under signal temporal logic tasks and uncertain dynamics, IEEE Robotics and Automation Letters 7 (4) (2022) 11561–11568. doi:10.1109/LRA.2022.3200760.